

**INTRAVAL Working Group 2 summary  
report on Phase 2 analysis of the  
Finnsjön test case**

Peter Andersson (ed.)<sup>1</sup>, Anders Winberg (ed.)<sup>2</sup>

- 1 GEOSIGMA, Uppsala, Sweden
- 2 Conterra, Göteborg, Sweden

January 1994

INTRAVAL WORKING GROUP 2 SUMMARY REPORT ON PHASE 2  
ANALYSIS OF THE FINNSJÖN TEST CASE

Peter Andersson (ed.)<sup>1</sup>, Anders Winberg (ed.)<sup>2</sup>

- 1 GEOSIGMA, Uppsala, Sweden
- 2 Conterra, Göteborg, Sweden

January 1994

This report concerns a study which was conducted for SKB. The conclusions and viewpoints presented in the report are those of the author(s) and do not necessarily coincide with those of the client.

Information on SKB technical reports from 1977-1978 (TR 121), 1979 (TR 79-28), 1980 (TR 80-26), 1981 (TR 81-17), 1982 (TR 82-28), 1983 (TR 83-77), 1984 (TR 85-01), 1985 (TR 85-20), 1986 (TR 86-31), 1987 (TR 87-33), 1988 (TR 88-32), 1989 (TR 89-40), 1990 (TR 90-46), 1991 (TR 91-64) and 1992 (TR 92-46) is available through SKB.

Client: **SKB**  
Grap: 94 001  
1994-01-17

**INTRAVAL WORKING GROUP 2 SUMMARY  
REPORT ON PHASE 2 ANALYSIS OF THE  
FINNSJÖN TEST CASE**

edited by

Peter Andersson, GEOSIGMA  
Anders Winberg, Conterra

Uppsala and Göteborg

January 1994

## **ABSTRACT**

A comprehensive series of tracer tests on a relatively large scale have been performed by SKB at Finnsjön, Sweden, to increase understanding of transport phenomena which govern migration of radionuclides in major fracture zones. The experimental sequence of tracer tests consisted of; a preliminary tracer test during hydraulic interference tests, a radially converging test and a dipole test. Both sorbing and slightly sorbing tracers were used. The conducted experiments were subsequently selected as a test case in the international INTRAVAL Project, in part because the tests at Finnsjön invite to direct address of validation of geosphere models. This report summarizes the study of the Finnsjön test case within INTRAVAL Phase 2, which has involved nine project teams from seven countries. Porous media approaches in two dimensions dominated, although some project teams utilized one-dimensional transport models, and even three-dimensional approaches on a larger scale. The dimensionality employed did not appear to be decisive for the ability to reproduce the observed field responses. It was also demonstrated that stochastic approaches can be used in a validation process. Only four out of nine project teams studied more than one process. The general conclusion drawn is that flow and transport in the studied zone is governed by advection and that hydrodynamic dispersion is needed to explain the breakthrough curves. Matrix diffusion is assumed to have small or negligible effect. The performed analysis is dominated by numerical approaches applied on scales on the order of a 1000m. Taking scale alone into account, the results of most teams are possible to compare. A variety of validation aspects have been considered. Five teams utilized a model calibrated on one test, to predict another, whereas the two teams utilizing stochastic continuum approaches addressed; 1) validity of extrapolation of a model calibrated on one transport scale to a larger scale, 2) performance assessment implications of choice of underlying distribution model for hydraulic conductivity, respectively.

## ABSTRACT (SWEDISH)

Ett antal spår försök har genomförts i stor skala av SKB vid Finnsjön för att öka förståelsen av transportprocesser som bestämmer migration av radionuklider i större sprickzoner. Sekvensen av spår försök omfattade; preliminära spår försök i samband med hydrauliska interferenstester, ett radiellt konvergerande försök och ett dipolförsök. Både icke sorberande och svagt sorberande spårämnen utnyttjades. De utförda experimenten valdes senare ut som ett testfall inom ramen för det internationella INTRAVAL-projektet, delvis beroende på att försöken i Finnsjön inbjuder till analys av möjligheten att validera modeller som beskriver flöde och transport i kristallint berg. Föreliggande rapport sammanfattar analysen av spår försöken i Finnsjön som utförts inom ramen för INTRAVAL Fas 2, som innefattar analys av nio projektgrupper från sju länder. Tvådimensionella modellansatser som bygger på porösa medier överväger, även om några grupper utnyttjat endimensionella transportmodeller, och till och med tredimensionella modeller i större skala. Dimensionaliteten i den valda ansatsen verkar dock inte vara avgörande för att kunna reproducera observerade responser i fält. Det demonstrerades också att stokastiska ansatser kan utnyttjas i en valideringsprocess. Bara fyra av nio projektgrupper studerade mer än en transportprocess. De övergripande slutsatser som drogs av grupperna var att flöde och transport i den studerade sprickzonen bestäms av advektion, och att hydrodynamisk dispersion krävs för att förklara i fält uppmätta genombrottskurvor. Matrisdiffusion antas ha en liten eller försumbar effekt på resultaten. Den utförda analysen domineras av numeriska ansatser på en skala av i storleksordningen 1000m. Om hänsyn enbart tas till den utnyttjade skalan så är det möjligt att jämföra resultaten från de flesta projektgrupperna. Olika aspekter på validering behandlas av de olika grupperna. Fem av grupperna utnyttjade en modell, kalibrerad mot ett spår försök, för att därefter prediktera ett annat försök, medan två grupper utnyttjade stokastiska kontinuumansatser för att behandla; 1) giltigheten i att extrapolera en modell kalibrerad på en transportskala, till en annan, större skala, respektive 2) funktions- och säkerhetsaspekter på valet av statistisk fördelningsfunktion för hydraulisk konduktivitet.

**TABLE OF CONTENTS**

	<u>Page</u>
<b>SUMMARY</b>	iii
<b>1 INTRODUCTION</b>	1
1.1 BACKGROUND	1
1.2 WORK PERFORMED IN PHASE 1	2
1.3 WORK PERFORMED IN PHASE 2	3
<b>2 DESCRIPTION OF THE FINNSJÖN EXPERIMENTS</b>	5
2.1 DESCRIPTION OF THE SITE	5
2.2 EXPERIMENTAL DESIGN	6
2.2.1 Hydraulic Interference Tests and Preliminary Tracer Test	6
2.2.2 Radially Converging Experiment	6
2.2.3 Dipole Tracer Experiment	7
2.2.4 Complementary Experiments	8
<b>3 SUMMARIES OF PROJECT TEAM ANALYSES</b>	13
3.1 SUMMARY OF GEOSIGMA/SKB ANALYSIS	13
3.1.1 Modelling Objectives	13
3.1.2 Modelling Approach	13
3.1.3 Results	14
3.1.4 Conclusions	16
3.2 SUMMARY OF VTT/TVO ANALYSIS	19
3.2.1 Modelling Objectives	19
3.2.2 Modelling Approach	19
3.2.3 Results	20
3.2.4 Conclusions	20
3.3 SUMMARY OF PNC ANALYSIS	26
3.3.1 Modelling Objectives	26
3.3.2 Modelling Approach	26
3.3.3 Results	26
3.3.4 Conclusions	27
3.4 SUMMARY OF PSI/NAGRA ANALYSIS	31
3.4.1 Modelling Objectives	31
3.4.2 Modelling Approach	31
3.4.3 Results	32
3.4.4 Conclusions	33
3.5 SUMMARY OF UNIVERSITY OF NEW MEXICO ANALYSIS	37
3.5.1 Modelling Objectives	37
3.5.2 Modelling Approach	37
3.5.3 Results	37
3.5.4 Conclusions	39

3.6	<b>SUMMARY OF HAZAMA CORPORATION ANALYSIS</b>	44
3.6.1	Modelling Objectives	44
3.6.2	Modelling Approach	44
3.6.3	Results	45
3.6.4	Conclusions	45
3.7	<b>CONTERRA/KTH-WRE ANALYSIS</b>	47
3.7.1	Modelling Objectives	47
3.7.2	Modelling Approach	47
3.7.3	Results	48
3.7.4	Conclusions	49
3.8	<b>BRGM/ANDRA ANALYSIS</b>	51
3.8.1	Modelling Objectives	51
3.8.2	Modelling Approach	51
3.8.3	Results	52
3.8.4	Conclusions	53
3.9	<b>UPV/ENRESA ANALYSIS</b>	57
3.9.1	Modelling Objectives	57
3.9.2	Modelling Approach	57
3.9.3	Results	58
3.9.4	Conclusions	58
4	<b>COMPARATIVE DISCUSSION</b>	61
4.1	GENERAL	61
4.2	CONCEPTUAL APPROACHES	61
4.3	PROCESSES STUDIED	62
4.4	SCALE OF APPLICATION	63
4.5	VALIDATION ASPECTS	63
5	<b>REFERENCES</b>	66

## SUMMARY

A comprehensive series of tracer tests on a relatively large scale have been performed by SKB at Finnsjön, Sweden, to increase the understanding of transport phenomena which govern migration of radionuclides in major fracture zones. The results are planned to be used to calibrate and verify radionuclide transport models. The experiments are focused on a low-angle, 100m thick fracture zone featured by a number of thin, highly conductive horizons interbedded with fairly low-conductive rock. One of the conductors which constitutes the upper boundary of the zone, is continuous over a larger distance, and also constitutes a chemical interface between saline waters at depth and freshwater above. The experimental sequence of tracer tests consisted of; a preliminary tracer test during hydraulic interference tests, a radially converging test and a dipole test. The radially converging involves one withdrawal hole and injection of 11 different tracers in different sections in three peripheral boreholes whereas the dipole test involves injection withdrawal in the uppermost conductive horizon using recirculation with intermediate observations in two flanking boreholes. Both non-sorbing and slightly sorbing tracers were utilized in the experiments.

The conducted experiments were subsequently selected as a test case in the international INTRAVAL Project based on the fact that many processes which govern geosphere transport on a larger scale are incorporated in the design and outcome of the tests. In addition the sequence of tracer tests at Finnsjön also invite to address directly the question of validation of geosphere models, which is the ultimate objective of the INTRAVAL study. The Work on the Finnsjön test case during Phase 1 of INTRAVAL involved models (10 in total) which ranged from simple advection-dispersion to more complex discrete fracture network models. It was found that most models were able to reproduce some breakthrough curves, at least. It was concluded that tracer test data from one to two tests are not sufficient to discriminate between models (processes). Inability to predict a tracer test on the basis of existing tracer test data was attributed to difficulties to incorporate the heterogeneity in Zone 2. The study of the Finnsjön test case was prolonged within Phase 2 of INTRAVAL which had its main focus on field experiments. Nine project teams from seven countries further studied and analyzed the data; GEOSIGMA (S), VTT (SF), PNC (J), PSI (CH), UoNM (USA), HAZAMA (J), Conterra/KTH-WRE (S), BRGM (F) and UPV (E).

This report summarizes the modelling objectives, modelling approaches, results, and conclusions of the project teams. In a discussion section the results are compared with regard to; conceptual approach taken, processes studied, scale of application and validation aspect of experiments considered. Compared to the Phase 1 analysis, the analysis performed in Phase 2 offer; more attempts on validation issues, three-dimensional analysis and applica-



tion of stochastic approaches. Porous media concepts dominate, the exception being two teams, which apply a channel network model and the crack tensor theory, respectively. Some teams even compare different conceptual approaches. Most applied models are two-dimensional which comes natural with the two-dimensional flow assumed to prevail in Zone 2. Some project teams utilize one-dimensional transport models, and two teams employ three-dimensional approaches. The dimensionality employed in the analysis does not, however, appear to be decisive for the ability to reproduce field responses at Finnsjön. A major difference compared to the Phase 1 analysis is that stochastic approaches are employed by three project teams. It was demonstrated that stochastic approaches can be used in a validation process, but that the question remains how to formally validate a stochastic model.

During the Phase 1 analysis, most teams studied several processes and tried to discriminate between them. This exercise indicated that the conducted tracer experiments may not be designed to make the desired discrimination. In the Phase 2 analysis only four out of nine project teams studied more than one process, e.g. only two teams consider sorption. This should be compared with the highly varying stand with regard to matrix diffusion taken as an outcome of the Phase 1 analysis. The general conclusion drawn by most teams is that flow and transport in Zone 2 is governed by advection and that hydrodynamic dispersion is needed to explain the breakthrough curves. Manifestation of matrix diffusion, or not, remains an open question although most teams consider it to have small or negligible effect given the high induced flow velocities and low ratio of fracture to matrix porosity.

In contrast to the Phase 1 analysis which mainly consisted of analytical approaches applied on the experimental scale of the Finnsjön tracer tests (~ 200m), the Phase 2 analysis is dominated by numerical approaches applied on significantly larger scales (~ 1000m). The two stochastic continuum approaches even consider transport phenomena on scales larger than the actual experiment scale. Taking scale alone into account, the results of most teams are possible to compare.

During Phase 1, three out of seven teams formally addressed validation by predicting the dipole test using a model calibrated using the radially converging test. During Phase 2, a variety of validation aspects have been considered. Five teams utilized variations of the above "classical" approach, whereas the two teams utilizing stochastic continuum approaches addressed; 1) validity of extrapolation of a model calibrated on one transport scale to a larger scale, 2) performance assessment implications of choice of underlying distribution model of hydraulic conductivity, respectively.

# 1 **INTRODUCTION**

## 1.1 **BACKGROUND**

The flow and transport of solutes in crystalline bedrock is to a large extent governed by the distribution of fractures and fracture zones in the bedrock as they constitute the main pathways for groundwater flow. The localization and characterization of potential pathways are essential for the safety assessment analyses of a repository for spent nuclear fuel.

The need of an increased knowledge regarding geological, hydrogeological, and geochemical characteristics of fracture zones, and the variation of these characteristics in time and space, made it necessary to investigate a fracture zone in more detail. Of special interest for the safety of a repository, placed in the vicinity of a fracture zone, is the flow and transport of solutes in the "good" rock between the repository and the fracture zone as well as the characteristics of the fracture zone itself.

This INTRAVAL test case is based on three hydraulic interference tests and two tracer experiments performed in a major low angle fracture zone (Zone 2) at the Finnsjön research area located in northern Uppland in central Sweden /Andersson et al., 1989/, /Gustafsson et al., 1990/, /Andersson et al., 1990/, /Gustafsson & Andersson, 1991/, /Gustafsson & Nordqvist, 1993/, /Andersson (ed.), 1993/, /Andersson et al., 1993/. The main objectives with the experiments were to determine parameters important for the understanding of radionuclide transport in major fracture zones and to utilize the results for calibration and verification of radionuclide transport models. An additional objective was to develop and improve equipment and experimental methods for application in future field experiments.

These experiments were selected as a test case in the INTRAVAL project since they were designed to study phenomena important in geosphere transport such as advection, dispersion, channelling, dilution, matrix diffusion, heterogeneity on a rather large geometrical scale. The Finnsjön experiments constitute a very comprehensive geohydrologic data base for studies of groundwater flow and transport in a major fracture zone of fractured crystalline rock.

## 1.2 **WORK PERFORMED IN PHASE 1**

In Phase 1 of the INTRAVAL Project a total of seven project teams studied and analyzed the data to various degrees. In Table 1-1 a summary of the project teams and their conceptual models are presented.

The interpretation of the available hydraulic information was mainly made by the SGAB team and their interpretation was accepted by the other project teams as being generally valid. Most of the other analyses were concentrated on interpreting the available tracer test data. A number of different conceptual models were applied ranging from simple linear advective–dispersive systems to more complex fracture network systems.

Table 1–1. Summary of modelling performed within Phase 1 of INTRAVAL.

Team	Representation	Dimension	Some of the effects considered
SGAB	Porous medium with sub-regions	2D	Dispersion Sorption Radioactive decay
	Linear advective dispersive system	1D	Dispersion Multiple flow paths
Intera	Horizontal constant aperture fracture allowing radial advection and dispersion	2D	Dispersion Two parallel fractures
KTH	Linear advective dispersive system	1D	Dispersion
	Linear advective dispersive system with matrix diffusion	1D	Dispersion Matrix diffusion
VTT	Channels	2D	Advective diffusion Generalized Taylor dispersion Multiple flow paths
JAERI	Variable–aperture fracture with channeling effect	2D	Advective dispersion Local dispersion Multiple flow paths Matrix diffusion
	Porous medium	2D	Advective dispersion Matrix diffusion
Hazama	Fracture network (3 subregions)	2D	Advective dispersion Matrix diffusion Multiple flow paths
EMP	Multiple channels	2D	Advective dispersion Multiple flow paths

The modelling showed that most of the models were able to fairly well reproduce at least some of the breakthrough curves. However, the results also showed that none of the models managed to fit all breakthrough curves entirely satisfactory. Since this partial success was accomplished one may conclude that the tracer test data from one or two tests alone are insufficient, by themselves, to distinguish between different models.

Another conclusion from Phase 1 is that none of the models were able to entirely "predict" one tracer test based on another. Several modelling teams suggested that reason for this was the difficulty to incorporate the heterogeneity of Zone 2 based on the available data.

### 1.3 WORK PERFORMED IN PHASE 2

The Finnsjön experiments were also selected as a test case for Phase 2 of the INTRAVAL study. One reason being that none of the teams in Phase 1 had been able to use the entire data set during Phase 1. Another reason was that Phase 2 was focused on field experiments and that the Finnsjön experiments constitutes one of the largest data bases for large scale transport in fracture crystalline rock.

Nine project teams from seven countries, including the Pilot Group (GEO-SIGMA) who developed this test case, studied and analyzed the data. Two of the groups were also participating in Phase 1, GEOSIGMA (former SGAB) and VTT. The project teams were:

1. GEOSIGMA, Sweden
2. Technical Research Centre of Finland (VTT)
3. Power Reactor and Nuclear Fuel Development Corporation (PNC),  
Japan
4. Paul Scherrer Institut (PSI), Switzerland
5. University of New Mexico (UNM), USA
6. Hazama Corporation, Japan
7. Conterra/Royal Institute of Technology (KTH), Sweden
8. Bureau de Recherches Géologiques et Minières (BRGM), France
9. Universidad Politecnica de Valencia (UPV), Spain

The processes studied and the conceptual approaches for the nine teams are summarized in Table 1-2.

Table 1-2. Phase 2 analysis of tracer tests at Finnsjön. Conceptual approaches used and processes considered

Modelling team	Conceptual approach	Processes considered
Hazama Corp., Japan	crack tensor theory	advection
Conterra/Water Res. Eng.(KTH), (SKB) Sweden	stochastic continuum multiGaussian	advection
BRGM (ANDRA),	continuum model	advection–dispersion kinematic dispersion radioactive decay
GEOSIGMA, (SKB), Sweden	continuum model	advection–dispersion diffusion sorption matrix diffusion radioactive decay
VTT (TVO), Finland	non–interacting varying aperture channel model	advective diffusion matrix diffusion gen. Taylor dispersion multiple flow paths
PNC, Japan	dual porosity continuum model stream tube concept	advection–dispersion multiple flow paths
UPV (ENRESA), Spain	stochastic continuum multiGaussian non–multiGaussian	advection
PSI (NAGRA), Switzerland	dual porosity continuum model	advection–dispersion diffusion sorption matrix diffusion
U. of New Mex– ico, U.S.A.	single and dual porosity continuum model	advection–dispersion molecular diffusion matrix diffusion

## DESCRIPTION OF THE FINNSJÖN EXPERIMENTS

This section gives a brief description of the experiments done at the Finnsjön site. The data available for the modelling teams is thoroughly described in INTRAVAL Phase 1 Test Cases /SKI/NEA, 1991/.

### 2.1 DESCRIPTION OF THE SITE

The general geological, geophysical and hydrological characteristics of the Finnsjön study site have been summarized by Ahlbom et al. (1986, 1988) and Ahlbom & Smellie (1989). At the main investigation site two major fracture zones have been identified, the Brändan fracture zone, Zone 1, and a low-angle zone, Zone 2 (Figures 2-1, 2-2). The geohydrology of the site is dominated by these two highly conductive zones. Zone 1 has a NNE strike with a dip of about 75° to the east, and the thickness of the zone is about 20 m. The hydraulic conductivity varies between  $1 \cdot 10^{-6}$  to  $5 \cdot 10^{-5}$  m/s as compared to  $1 \cdot 10^{-7}$  m/s in the country rock (2 m test intervals).

Zone 2, which is the zone utilized for the tracer tests, is trending north with a dip of about 16° to the west and consists of sections with high fracture frequency and tectonisation. The zone is well defined in 7 boreholes located within an area of about 500×500 m (Figure 2-1). In this area the fracture zone is almost planar with the upper surface located between 100 to 240 m below ground. The zone is about 100 m thick and seems to consist of three subzones with hydraulic conductivities of  $2 \cdot 10^{-4}$ ,  $1 \cdot 10^{-4}$  and  $1 \cdot 10^{-5}$  m/s (2m test intervals) going from the uppermost zone downwards. The parts in between the subzones have hydraulic conductivities similar to the country rock. Within the fracture zone the mean value is  $5 \cdot 10^{-6}$  m/s. The direction of the groundwater gradient in Zone 2 is towards ENE, and varies in magnitude from 1m/350m to 1m/150m.

The rock where Zone 2 is located is dominated by granodiorite. The rock is medium-grained and red in color. The fracture infillings are dominated by calcite. Other minerals present are hematite, laumontite, asphaltite and clay minerals.

The composition of the groundwater above Zone 2 differs from that in and below Zone 2. The water above the zone is a younger near-surface water, and the water below Zone 2 is an old saline water characterized by a high content of species in solution such as Na, Ca and Cl. The water in Zone 2 is a mixture of these two waters which indicates the appearance of two circulating groundwater systems, one above and one below Zone 2. Both are drained into Zone 2 in the area where Zone 2 is most deeply located and the water is discharged from the shallow parts of Zone 2 into Zone 1.

## 2.2 EXPERIMENTAL DESIGN

### 2.2.1 Hydraulic Interference Tests and Preliminary Tracer Test

Three hydraulic interference tests were carried out by withdrawal from different isolated intervals in borehole BFI02 within Zone 2, i.e. the lower and upper parts (test 1 and 2, respectively) and from the entire zone (test 3B) /Andersson et al., 1989/ (Figure 2-3).

The pressure responses were registered in 3-6 intervals in all boreholes in the Brändan area and also in 6 boreholes outside the Brändan area up to 1500 m from the pumping well. During the tests, the flow rate of the discharged water during pumping, electrical conductivity and temperature of the discharged water and the atmospheric pressure were also measured. Registrations of the groundwater table in the observation holes were also undertaken.

During interference test 2 a preliminary tracer test was performed in order to optimize the design and performance of the planned radially converging experiment. Tracers were injected as pulses in the upper highly conductive subzone of Zone 2 in boreholes BFI01, KFI06 and KFI11. Tracer breakthroughs were monitored in the pumping well BFI02.

### 2.2.2 Radially Converging Experiment

In the radially converging experiment borehole BFI02 was used as a withdrawal hole and injection of tracers into Zone 2 was made in three peripheral holes, BFI01, KFI06 and KFI11 (Figures 2-1, 2-2) /Gustafsson et al., 1989/. In each injection hole three sections were packed off, one in the upper highly conductive part of Zone 2, one at the lower boundary of Zone 2 and one at the most highly conductive part in between. In the withdrawal hole the packed-off section enclosed the whole thickness of Zone 2.

In total 11 different tracers were injected, 8 of them continuously for 5-7 weeks, and three as pulses. The injection intervals in each injection hole and the tracers injected are given in Table 2.1. The tracers selected, DTPA- and EDTA complexes, fluorescent dyes and anions, are stable and non-sorbing.

During the continuous pulse injection the injection flow rate was registered as injected volume of tracer solution versus time. The water volume discharged from the injection system was also measured and sampled in order to determine the tracer concentration in the injection section. Pulse injections of tracers were performed after the continuous injection of tracers had been terminated.

Table 2-1. Injection intervals and tracers used in the radially converging experiment.

Hole	Interval (m)	Tracer	Type of Injection
BFI01	Upper; 241.5 – 246.5	In-EDTA	Continuous
	Middle; 263.5 – 266.5	Uranine	Continuous
	Lower; 351.5 – 356.5	Ho-EDTA	Continuous
KFI06	Upper; 212.0 – 217.0	Iodide	Pulse
	Middle; 236.5 – 239.5	Yb-EDTA	Continuous
	Lower; 252.5 – 271.5	ReO <sub>4</sub>	Continuous
KFI11	Upper; 221.5 – 226.5	Gd-DTPA	Continuous
		Tm-EDTA	Pulse
		Amino G	Pulse
	Middle; 282.5 – 294.5	Er-EDTA	Continuous
	Lower; 329.5 – 338.5	Dy-EDTA	Continuous

The tracer was withdrawn by pumping at a rate of 2.0 l/s in hole BFI02 from a packed-off section covering the whole thickness of Zone 2. The water discharged from the hole was continuously sampled for tracer analysis during the time period of tracer injection. The hydraulic head in the pumped section and also the groundwater level was registered. After the end of tracer injection a detailed sampling of the withdrawal hole was made in order to determine possible interconnections between highly conductive intervals of Zone 2. After the detailed sampling, the withdrawal and sampling of water from the entire thickness of Zone 2 was continued.

### 2.2.3 Dipole Tracer Experiment

The dipole experiment was performed in a recirculating system between BFI01 (injection) and BFI02 (withdrawal) /Andersson et al., 1990, 1993/. Holes KFI06 and KFI11 were used as observation holes.

In the dipole experiment only the upper highly conductive part of Zone 2 was used for tracer injection in hole BFI01, the same upper section as was used in the radially converging experiment. The two observation holes were packed-off in the same manner as in the radially converging test. Water from the packed-off section in the withdrawal hole BFI02 was recirculated to the injection section in BFI01 through a pipe system and tracers were injected into the system were the pipe entered the injection hole (Figure 2-4). Two tracer injections were also made in the upper section of the observation hole KFI11.



In total 15 injections of tracers were made during 7 weeks. Both radioactive and nonradioactive tracers were used. The radiotracers included both non-sorbing and sorbing species. The tracers were sampled in the upper part of Zone 2 in holes BFI02 and KFI11 with automatic samplers in the same way as in the radially converging test. Occasionally, samples were also taken in the water from the lower intervals of hole KFI11 and in the water from the sections in hole KFI06.

For the sorbing tracers the chemistry of the circulating water is of importance and therefore a comprehensive chemical analysis of the sampled water was made at the end of the dipole experiment. During the experiment the temperature of the water entering the injection hole BFI01 and the oxidation-reduction potential were measured showing that the conditions were stable and reducing. The electrical conductivity and the temperature of the water discharged from the withdrawal hole BFI02 were registered every day during the experiment.

During the pumping period the pumping rate was measured once a day. Hydraulic heads in 9 different boreholes in the area were measured almost every day during the pumping period and measurements were also made prior to the start of the dipole pumping and one week after terminating the pumping.

#### 2.2.4 **Complementary Experiments**

Laboratory measurements of the porosity and diffusivity were performed on drillcore samples from boreholes KFI06 and KFI11 /Gidlund et al., 1988/. The samples were taken at different distances from a fracture surface. The porosity was determined from the difference in dry and wet weight of the sample. The diffusivity was determined by placing a sample between two reservoirs, one containing a tracer solution (Iodide or Uranine) and the other initially free from tracer, and measuring the concentration increase of the tracer in the low concentration reservoir.

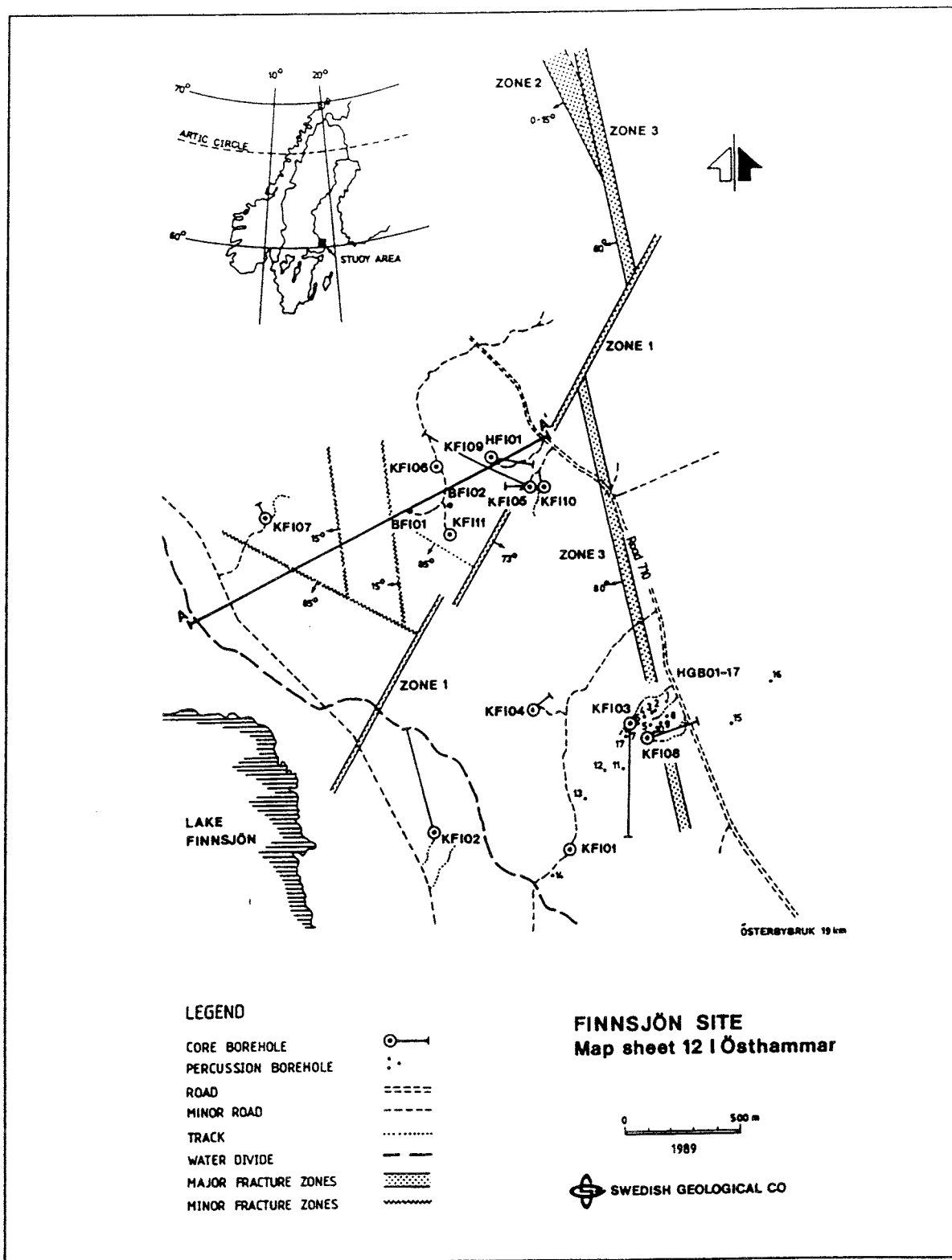


Figure 2-1. Finnsjön site, location of boreholes and major fracture zones. From Ahlbom & Smellie (1989).

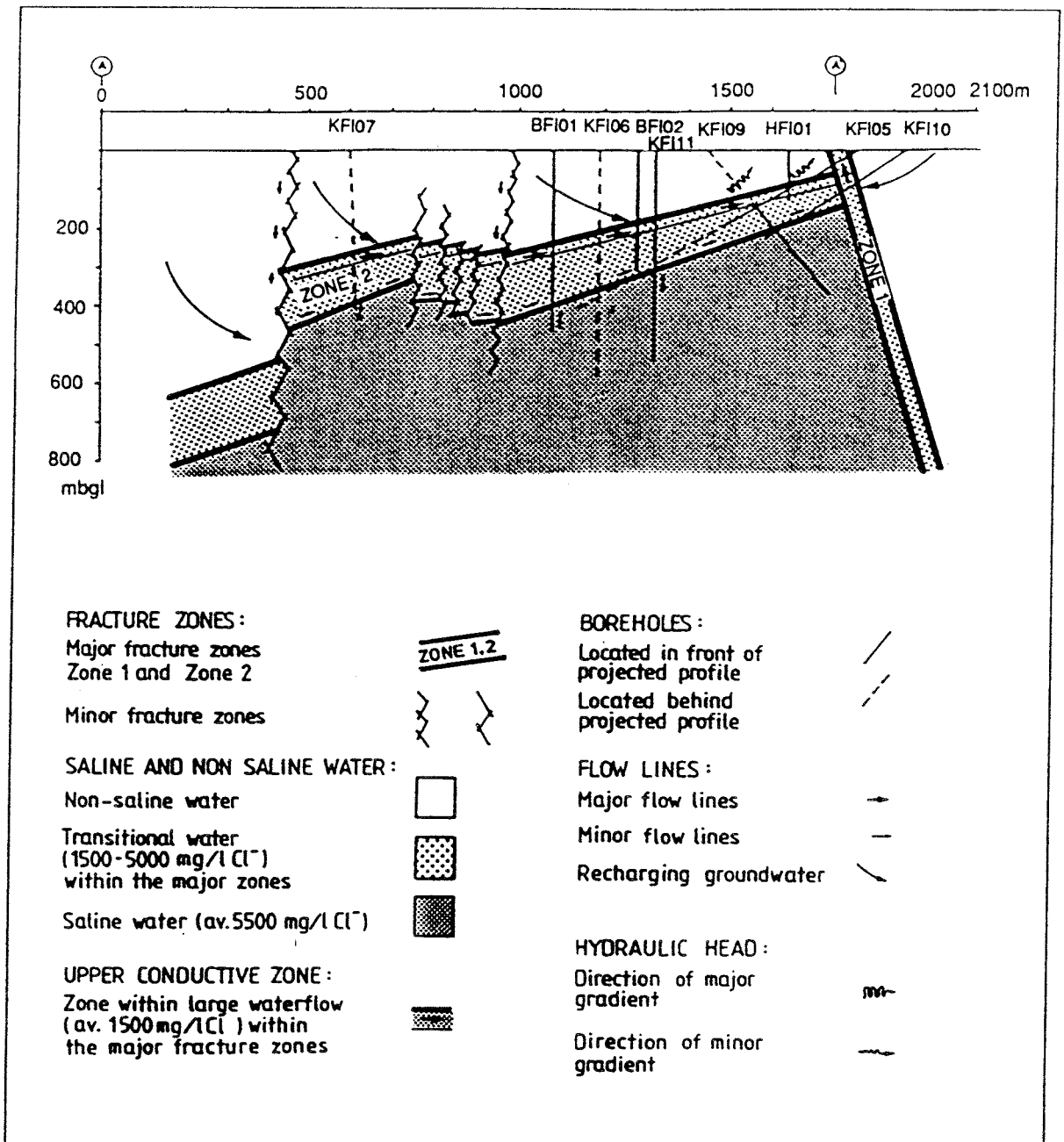


Figure 2-2. Cross-section through the Brändan area showing Zone 2. Profile A-A' is shown in Figure 2-1. From Ahlbom & Smellie (1989).

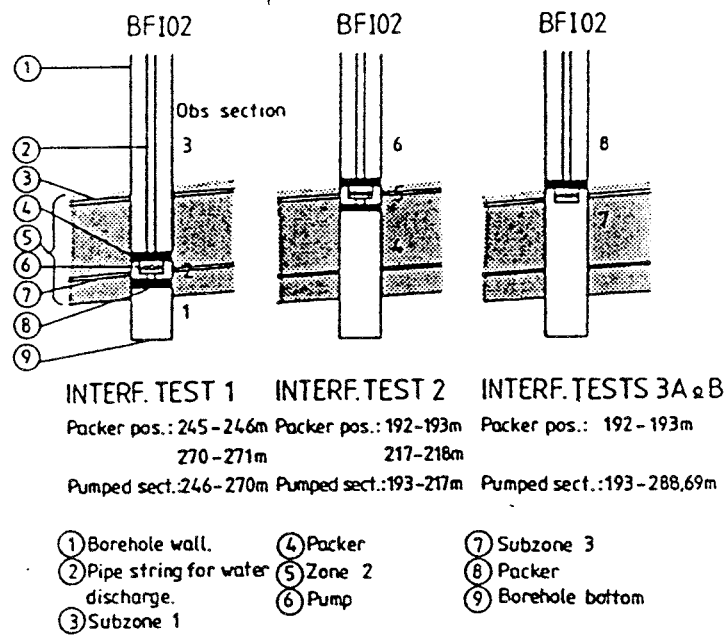


Figure 2-3. Schematic illustration of the experimental design in the pumping hole BFI02 during the large scale interference tests. From Andersson et al. (1989).

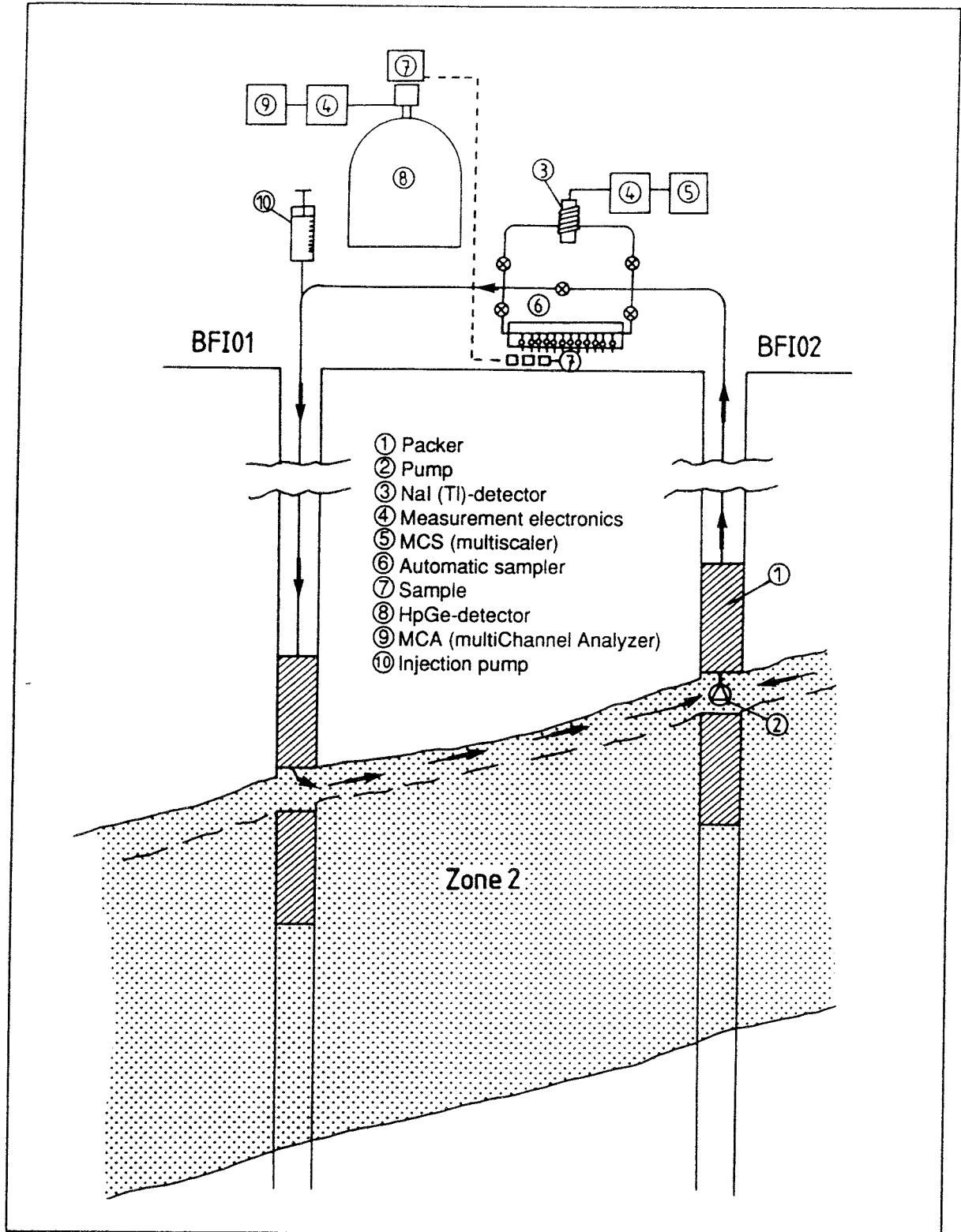


Figure 2-4. Experimental design of the dipole experiment. From Andersson et al. (1993).

### 3 SUMMARIES OF PROJECT TEAM ANALYSES

#### 3.1 SUMMARY OF GEOSIGMA/SKB ANALYSIS

The GEOSIGMA/SKB analysis is a continuation of the original evaluation of the tracer experiments in Zone 2 presented during INTRAVAL Phase 1 /Tsang & Neuman (editors), 1992/. The intention of this work has not primary been to validate models but instead evaluate tracer methods and to determine averaged transport parameters for a major fracture zone in crystalline rock. This section is a summary of the analysis of the dipole experiment also presented in Andersson et al. (1993).

##### 3.1.1 Modelling Objectives

The general purpose for all the modelling was to predict each field experiment based on all available information and compare the results with the actual outcome of the experiment. As each experiment was completed, new information could be added to the model in order to improve the predictive ability for the prediction of the following experiment. It was emphasized during the this whole sequence that groundwater flow should be predicted as well as solute transport. In addition to the general modelling purpose described above, model simulations were also performed in order to assist in the design of all the different experiments.

The specific purpose of the two-dimensional modelling of the dipole experiment was to make a direct comparison with earlier predictions and experimental data. Variations of the magnitude and direction of the natural gradient as well as effects of anisotropy and leakage were also examined.

The one-dimensional modelling was made in order to evaluate and compare transport parameters for the breakthrough in the observation holes where the transport can be assumed to be one-dimensional. The evaluation also includes parameter estimates from two or more breakthrough curves simultaneously.

##### 3.1.2 Modelling Approach

For both the one-dimensional and the two-dimensional approaches a simple porous medium advection-dispersion model was applied. The breakthrough in the two observation holes KFI06 and KFI11 was modelled assuming constant fluid velocity and no transversal dispersion. The one-dimensional models were solved using analytical solutions as given by Van Genuchten & Alves (1982). Variable injection schemes were simulated by superposition of

these solutions.

The fitting was generally made for three parameters, dispersion coefficient,  $D$ , mean velocity,  $v$ , and proportionality factor,  $f$ . The  $f$ -parameter is the product of injection concentration, dilution in the sampling section, and a weight representing the contribution from each main flow path. The fitted parameters were transformed into the form of more conventional transport parameters: residence time,  $t_0$ , longitudinal dispersivity,  $\alpha_L$ , and Peclet number,  $Pe$ . The uniqueness of the parameter estimates was assessed by studying the regression statistics of each model run: the correlation coefficients, standard error of the parameters, and the correlation between the parameters. A classification was made on a scale from 1 to 3 where 1 represents a poor model, 2 represents an acceptable model, and 3 a good model.

The one-dimensional modelling also included determination of retardation coefficients for some of the weakly sorbing tracers using simultaneous fits of two or three breakthrough curves, one being conservative and the other(s) retarded.

The two-dimensional modelling was made in a 0.5 m thick horizontal plane of the fracture zone covering a region of 500 x 500 m. The transport equation was solved numerically by the 2D finite element code SUTRA /Voss, 1990/ with a discretization of 10 x 10 m (2500 elements). Simulations were made applying different natural gradients and anisotropy factors trying to simultaneously fit all three breakthrough curves using inverse modelling technique.

### 3.1.3 **Results**

The results of the one-dimensional analysis show that the transport between the injection hole and observation borehole KFI11 can be very well described with a single flow path model, see Figure 3-1. The regression statistics display high correlation coefficients, small standard errors and low correlation between the fitting parameters. In Table 3-1 a summary of the model runs for transport path BFI01-KFI11 is presented.

Table 3-1 shows that the variation in residence times and dispersivities is small for the non-sorbing tracers ( $^{82}\text{Br}^-$ ,  $^{186}\text{ReO}_4^-$ ,  $^{131}\text{I}^-$ ,  $^{169}\text{Yb-EDTA}$ , and  $^{58}\text{Co-EDTA}$ ) as indicated by the standard deviations.  $^{140}\text{La-DOTA}$ ,  $^{177}\text{Lu-DOTA}$  and Rhodamine WT are weakly sorbing and are markedly delayed. The determination of retardation coefficient using simultaneous parameter estimation of two or three curves showed values of 1.3-1.7, see Figure 3-2.

$^{51}\text{Cr-EDTA}$ ,  $^{111}\text{In-EDTA}$ , and  $\text{In-EDTA}$  (stable) also shows minor delays. Some of the tracers, e.g.  $^{24}\text{Na}^+$  and  $^{160}\text{Tb-EDTA}$ , are not delayed but shows lower peak values and less recovery than others indicating irreversible losses.

Table 3-1. One-dimensional model simulations of the transport between BFI01 and KFI11 during the dipole tracer test.

Transport path	Tracer	Run	$t_0$ (h)	D/v (m)	f	Class*	
BFI01-KFI11	$^{82}\text{Br}^-$	1	22.8	11.9	1.07	2	
		6	23.2	7.4	0.99	3	
	$^{186}\text{ReO}_4^-$	2	24.1	7.8	0.83	2	
		6	22.8	7.6	0.87	3	
	$^{131}\text{I}^-$	3	22.9	6.8	1.15	3	
		6	23.2	8.2	0.92	3	
		3+6	22.6	6.9	1.01	3	
	$^{24}\text{Na}^+$	6	22.6	5.5	0.50	2	
	$^{140}\text{La}$ -DOTA	7	33.0	17.3	0.93	2	
	$^{177}\text{Lu}$ -DOTA	7	44.0	25.7	0.91	2	
	$^{51}\text{Cr}$ -EDTA	7	24.6	10.0	0.86	3	
	$^{111}\text{In}$ -EDTA	7	24.7	10.2	1.02	2	
	$^{160}\text{Tb}$ -EDTA	7	22.2	9.2	0.44	2	
	$^{169}\text{Yb}$ -EDTA	7	22.8	7.7	1.11	3	
	$^{58}\text{Co}$ -EDTA	8	22.9	7.3	0.62	3	
	Rhodamine WT	A		30.5	20.8	1.26	1
		E		35.7	23.6	0.93	2
	In-EDTA	C		27.4	14.6	0.25	2
	Gd-DTPA	D		22.7	7.4	0.38	3
Tm-EDTA	D		23.4	9.9	0.42	3	
<b>Mean value (standard deviation)**</b>			<b>22.9 (0.22)</b>	<b>7.4 (0.48)</b>			

\* Classification of model: 1=poor, 2=acceptable, 3=good

\*\* Based only on non-sorbing tracers (Br, Re, I, Yb, Co) with classification 3.

The breakthrough in KFI06 is markedly delayed compared to KFI11. The long residence times only enabled detection of the rising part of the breakthrough curves. These model simulations are therefore more ambiguous and consequently classified as being poor. No attempts were made to determine retardation coefficients based on breakthrough data from KFI06 due to the lack of uniqueness of the model fits.

Andersson et al. (1993) also made a comparison of some parameters determined from all three tests using the same concept of linear advective dispersive transport. Table 3-2 presents the results from the two transport routes BFI01-BFI02 and KFI11-BFI02. The results indicate that dispersivity decreases with increased flow velocity. Andersson et al. (1993) also concludes that matrix diffusion is likely to have a negligible effect based on estimates of the ratio of fracture to matrix porosity.

The results of the two-dimensional modelling of the dipole experiment



shows that it is not possible to fit all three breakthrough curves in the pumping hole and observation holes by applying different magnitudes and directions of the natural gradient. Only minor improvements of the model fits was obtained. However, including an anisotropy factor ( $K_{\max}/K_{\min}$ ) of about 8 directed approximately along the strike of the zone, gives a remarkably good agreement between data and model for all three breakthrough curves, see Figure 3-3. The model fits are also slightly improved by including leakage from the lower parts of Zone 2, as indicated by independent information such as head and electrical conductivity data.

Table 3-2. Comparison of some flow and transport parameters determined from three different tracer experiments performed in the upper highly transmissive part of Zone 2.

Route	Parameter	Interference test	Dipole experiment	Radially converging experiment
	Q (l/min)	500	120	82
KFI11-BFI02 (two paths)	$\Delta h$ (m)	3.7	0.91	0.81
	$t_{01}$ (h)	8	27	39
	$t_{02}$ (h)	15	110	103
	$\alpha_{L1}$ (m)	2.7	5.5	3.6
	$\alpha_{L2}$ (m)	11.4	65	10.7
BFI01-BFI02 (one path)	$\Delta h$ (m)	5.3	2.7	1.1
	$t_0$ (h)	35	45	154
	$\alpha_L$ (m)	2.4	5	6.3

### 3.1.4

#### **Conclusions**

The analysis of the whole sequence of interference tests and tracer tests performed both in Phase 1 and Phase 2 of INTRAVAL shows that a relatively simple porous media advection–dispersion model fairly well can predict average flow and transport in Zone 2. However, for predicting transport to individual observation points within the flow field (as in the dipole experiment) there is a need for a better description of local heterogeneities. The use of the whole sequence of tests with predictions, calibration and verification has proved to be a useful way to obtain consistency.

The analysis of the dipole test using one- and two-dimensional porous media approaches shows that:

- Good fits and consistent parameter values are obtained for individual observation points within the dipole flow field.

- Simultaneous fits of two or three breakthrough curves gives good fits for weakly sorbing tracers applying a linear sorption isotherm.
- Only one flow path is needed to explain transport from BFI01 to KFI11 and KFI06 while two paths are needed for the transport between KFI11 and BFI02 which is consistent with previous modelling of the radially converging test.
- Including an anisotropy factor ( $K_{\max}/K_{\min}$ ) of about 8 directed approximately along the strike of the zone, gives a remarkably good agreement between data and model.

Finally, the comparison of parameter values determined from the one-dimensional analysis of three different tests shows that dispersivity decreases with increased flow velocity. Andersson et al. (1993) suggests that this is an effect of the induced flow geometry.

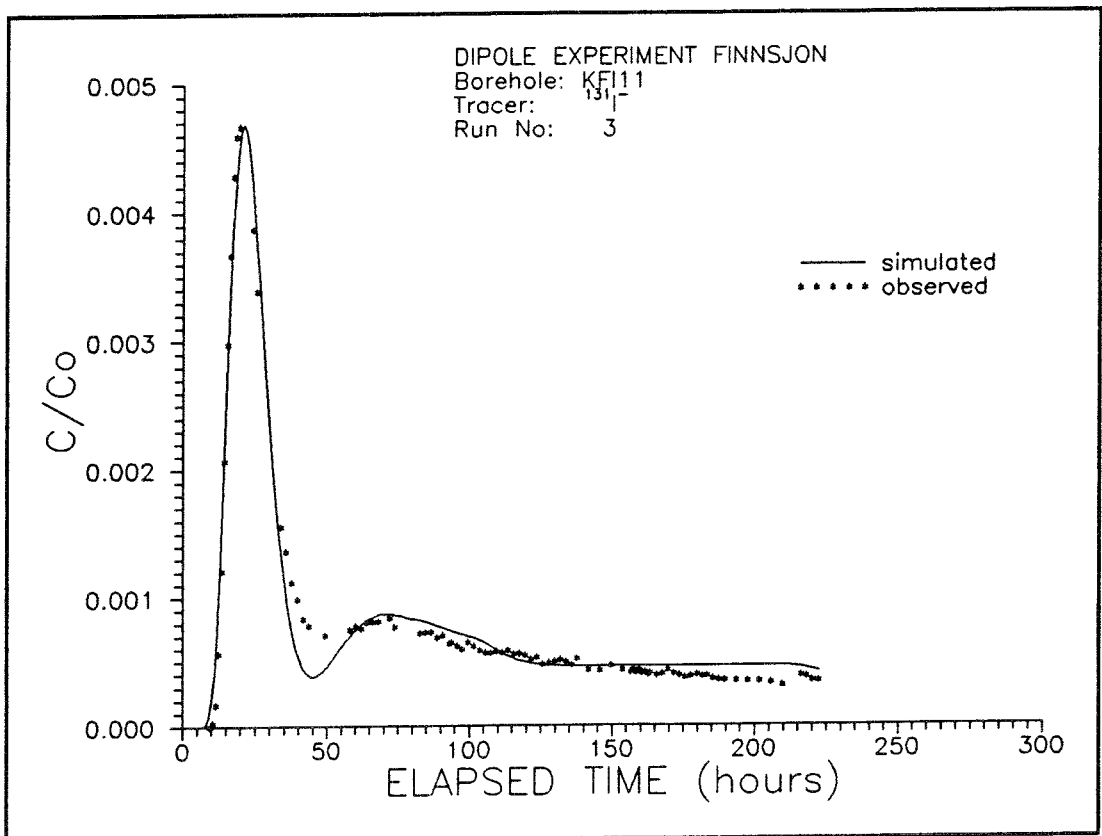


Figure 3-1. Simulated and observed breakthrough of Iodide in borehole KFI11 /Andersson et al., 1993/.

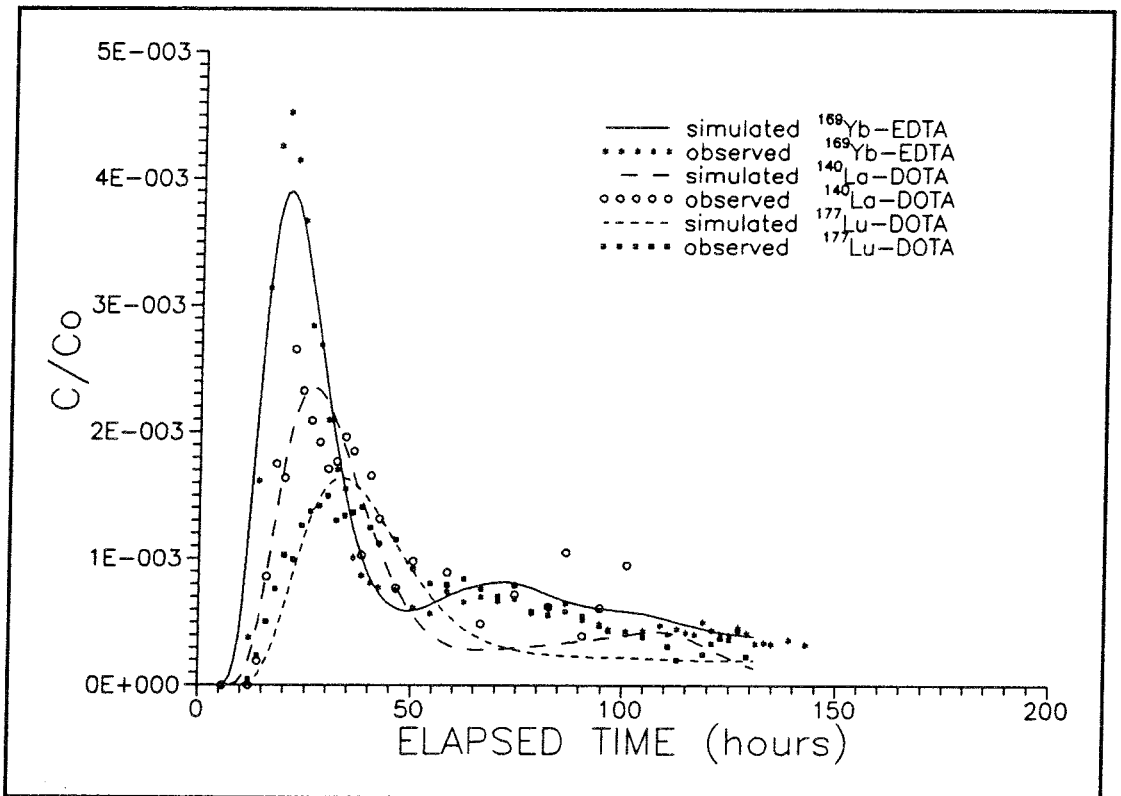


Figure 3-2. Simultaneous model simulation of breakthrough in borehole KFI11 for  $^{169}\text{Yb-EDTA}$ ,  $^{140}\text{La-DOTA}$ , and  $^{177}\text{Lu-DOTA}$  /Andersson et al., 1993/.

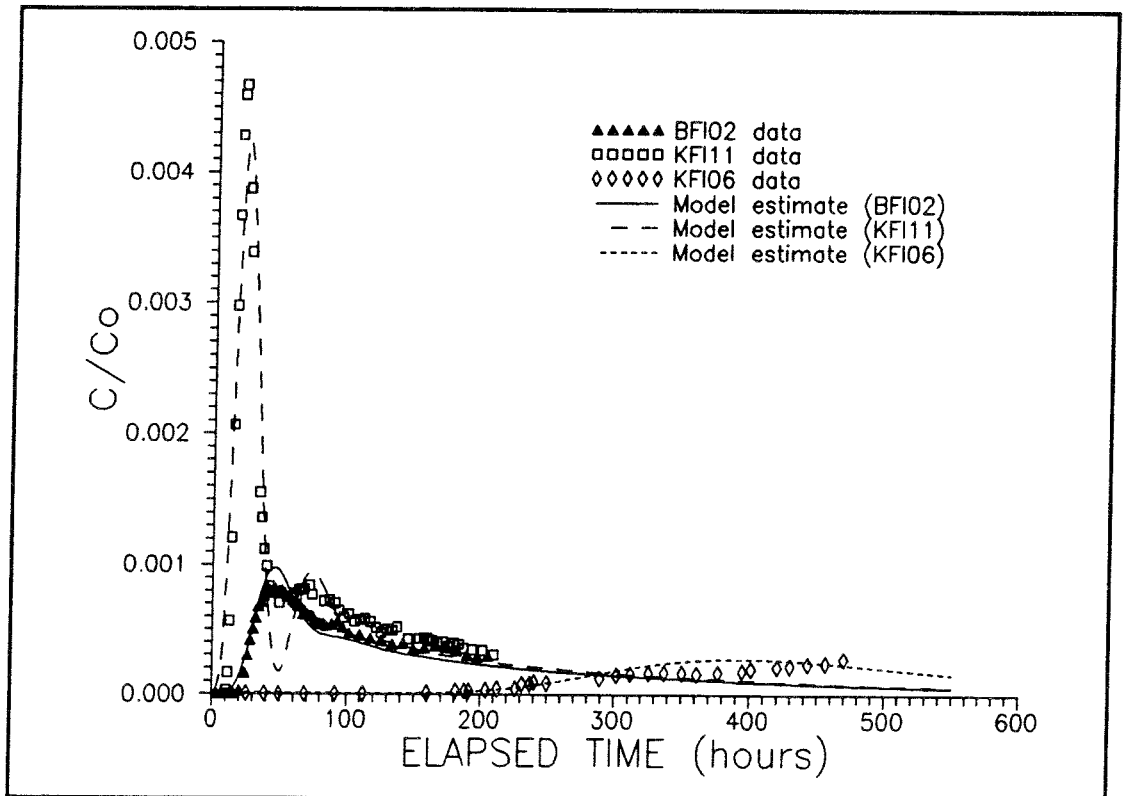


Figure 3-3. Results of estimation using data from all boreholes simultaneously, assuming anisotropic hydraulic conditions and aerially distributed vertical leakage. /Andersson et al., 1993/.

## 3.2 SUMMARY OF VTT/TVO ANALYSIS

The VTT/TVO analysis is a continuation of the work done within Phase 1 of the INTRAVAL Project. The work within Phase 1 included predictions and comparisons with the results of both the radially converging and the dipole experiments. Within Phase 2, also the preliminary tracer test performed in combination with the interference test was analyzed using the same conceptual model as for the other experiments.

### 3.2.1 **Modelling Objectives**

The overall objective of the VTT/TVO analysis was to obtain a model which is as realistic as possible for description of groundwater flow and transport in rock fractures and to put the right weights on processes affecting releases and mass fluxes.

For Phase 2 a specific objective was to investigate whether the same concept could be applied to all three experiments in Zone 2 at Finnsjön. Based on the results, conclusions regarding groundwater flow and transport are given together with general recommendations for future tracer tests in crystalline rock.

### 3.2.2 **Modelling Approach**

Within Phase 2, the same conceptual model for groundwater flow and tracer transport was adopted as within Phase 1 for the radially converging and dipole experiments. A concept of non-interacting, varying aperture channels was applied also in the continuation of the work. Water flow in a fracture is assumed to be concentrated in channels. The three-dimensional tortuous channels can conceptually be flattened and straightened into a two-dimensional channel network in a fracture plane. The channel network is assumed so dense that hydraulic radial symmetry is obtained during pumping, see Figure 3-4. It was also assumed that only one or two routes through fractures and channels contribute significantly to the transport from the injection section to the pumped borehole.

The apertures as well as the widths of the channels may vary strongly along the channel lengths. The aperture variation is taken into account in the transit time calculations. A mean effective width is assumed to describe the possibly varying width of each channel. For further details see Hautojärvi & Taivassalo (1988).

A linear flow velocity field across the channel width is used in the model. This approximation is thought to reveal most of the essential features of the coupling between velocity field and diffusion. The conceptual model for convective diffusion is illustrated in Figure 3-5.

The preliminary tracer test, performed in the same geometry as the radially converging experiment but with about 6 times higher pumping rate in the upper part of Zone 2, was simulated using one significant route and approximately the same channel widths as for the radially converging and dipole experiments where a channel width was fixed to 5 cm. In the evaluation of the preliminary tracer test the channel width was treated as a fitting parameter using fit by eye method.

### 3.2.3 **Results**

The results of the transport simulations, presented in Figures 3-6 to 3-8 show good agreement for two of the flow paths, KFI11-BFI02 and KFI06-BFI02 using approximately the same channel widths as for the radially converging and dipole experiment (5 cm), 3.1 and 4.2 cm respectively. However, for the transport between BFI01 and BFI02 the fit is somewhat ambiguous. The fit is either good in the rising part or in the tail depending on the channel width chosen, 6.58 cm or 1.70 cm. Taking into account differences in the performed experiments and uncertainties in the actual source terms the results can be considered to be essentially the same.

Hautojärvi (1992) also compares the two dominant transport processes in field tracer tests, hydrodynamic dispersion and matrix diffusion. By applying simple analytical solutions to the advection-dispersion and advection-matrix diffusion equations, respectively a relation between flow rate,  $Q$ , and the effective diffusion coefficient,  $D_e$ , was obtained (Figure 3-9).

In the Finnsjön experiments flow rates through the injection sections were at least in the order of ml/min and these experiments would thus be far on the dispersion dominated side in the plot.

### 3.2.4 **Conclusions**

The modelling, using a relatively simple channel approach, has shown that all three experiments performed in Zone 2 at Finnsjön, can be described with the same concept. Flow is dominated by advection and the only other process needed to explain the breakthrough curves is hydrodynamic dispersion. The high flow rates, measured from tracer dilution during the experiments, in combination with relatively slow transport indicate large cavities in the rock. The modelling has also shown that hydrodynamic dispersion can be described by velocity differences in a channel together with molecular diffusion.

Hautojärvi (1993) also concludes that the transport times within Zone 2 can be predicted reasonably well from hydraulic data e.g. by correcting the parallel plate interpretation of hydraulic data with a factor (possibly increasing with decreasing transmissivity).

Based on the comparison of hydrodynamic dispersion and matrix diffusion

presented above some conclusions for the INTRAVAL Project and for future experiments and "validation" exercises regarding matrix diffusion are /Hautojärvi, 1992, 1993/:

- Matrix diffusion is the most dominant process of far field transport in performance assessment.
- Matrix diffusion is extremely difficult (if not impossible) to measure in flow type field or laboratory experiments and should be measured in purely diffusion type experiments instead.
- Diffusion in the fracture plane may cause matrix diffusion like behavior.
- Advection-(Fickian) Dispersion-Matrix diffusion-models with a bulk flow velocity should not be used in the interpretation unless this kind of situation is ensured.
- Tracer experiments should aim at studying flow/channeling concepts, not at determining matrix diffusion parameters from breakthrough curves. The experiments should be performed with different flow velocities or distances for any kind of validation of transport models.

The VTT/TVO team has also made some general conclusions regarding tracer experiments and modelling based on the experiences from both phases of the INTRAVAL Project:

- Flow rate measurements together with tracer experiments are useful for concept and transport modelling but ambiguities still remain.
- Laboratory and field experiments seem to weigh processes differently compared to a performance assessment situation.
- It is very important to interpret the experimental situation right. Geometry and processes instead of "fitting parameters".
- Different models may be needed to evaluate experiments and to do performance assessment. A variety of models for different scales are needed and they have to be consistent with data and with each other.

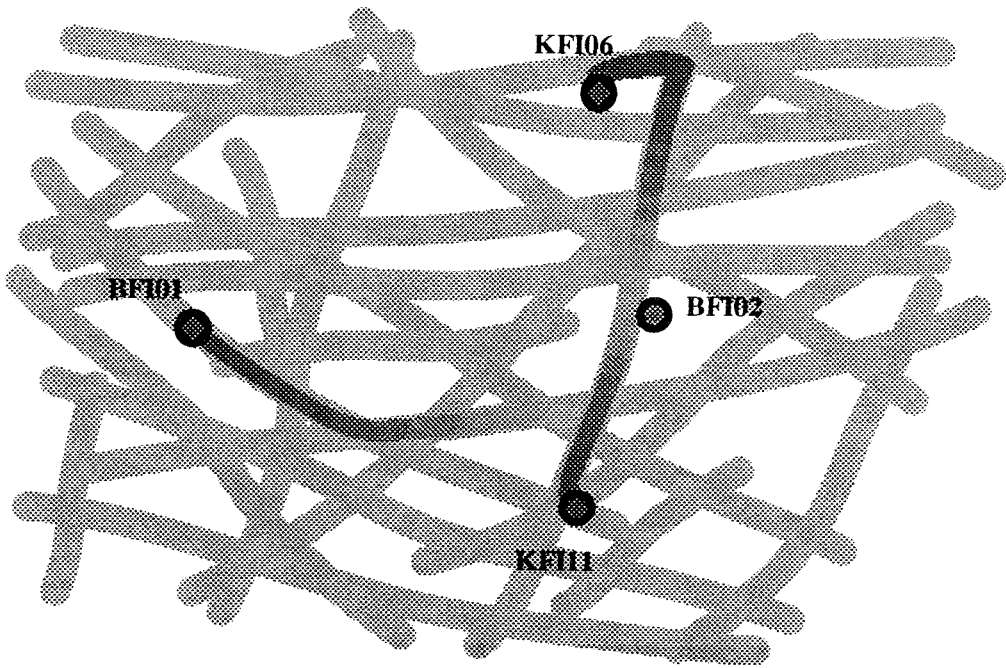


Figure 3-4. Conceptual model of channel network in a fracture plane.  
/Hautojärvi & Taivassalo, 1988/.

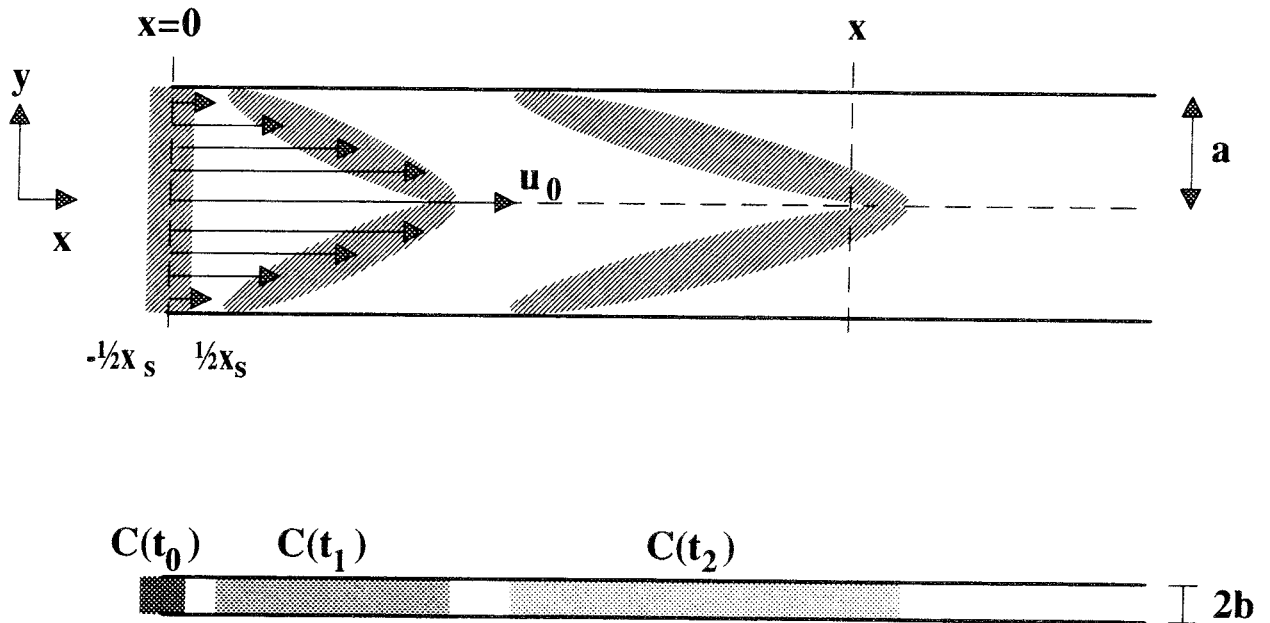


Figure 3-5. Convective diffusion of a tracer in a fracture channel.  
/Hautojärvi & Taivassalo, 1988/.

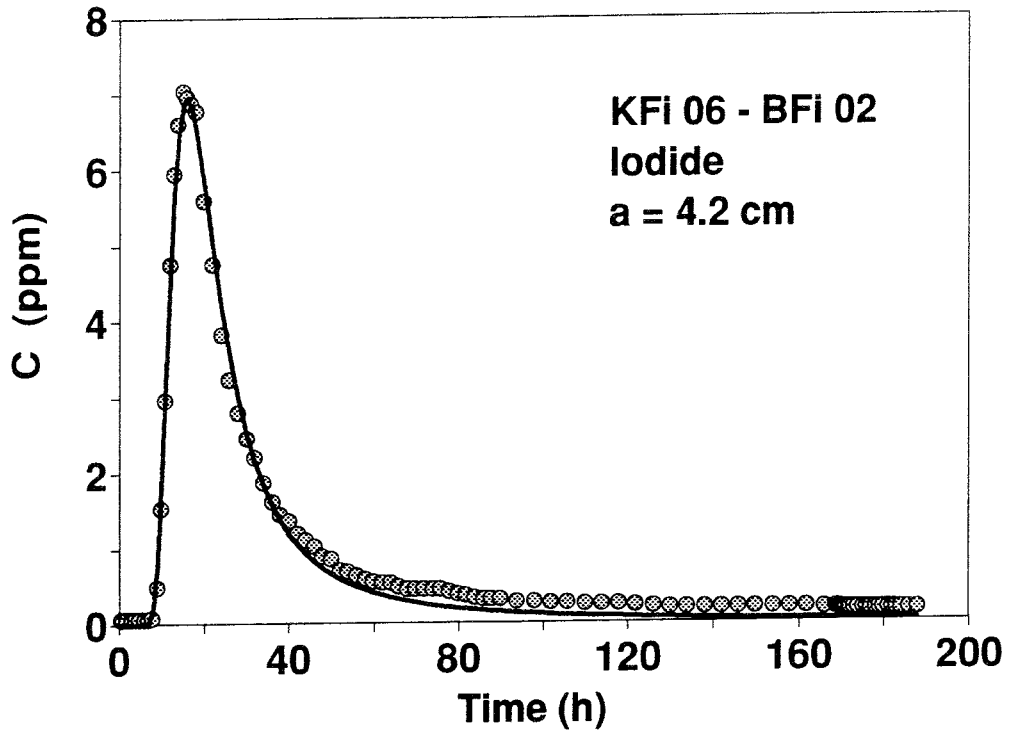


Figure 3-6. Observed and simulated (solid line) tracer breakthrough from injection in KFI06 during the preliminary tracer test. /Hautojärvi, 1993/.

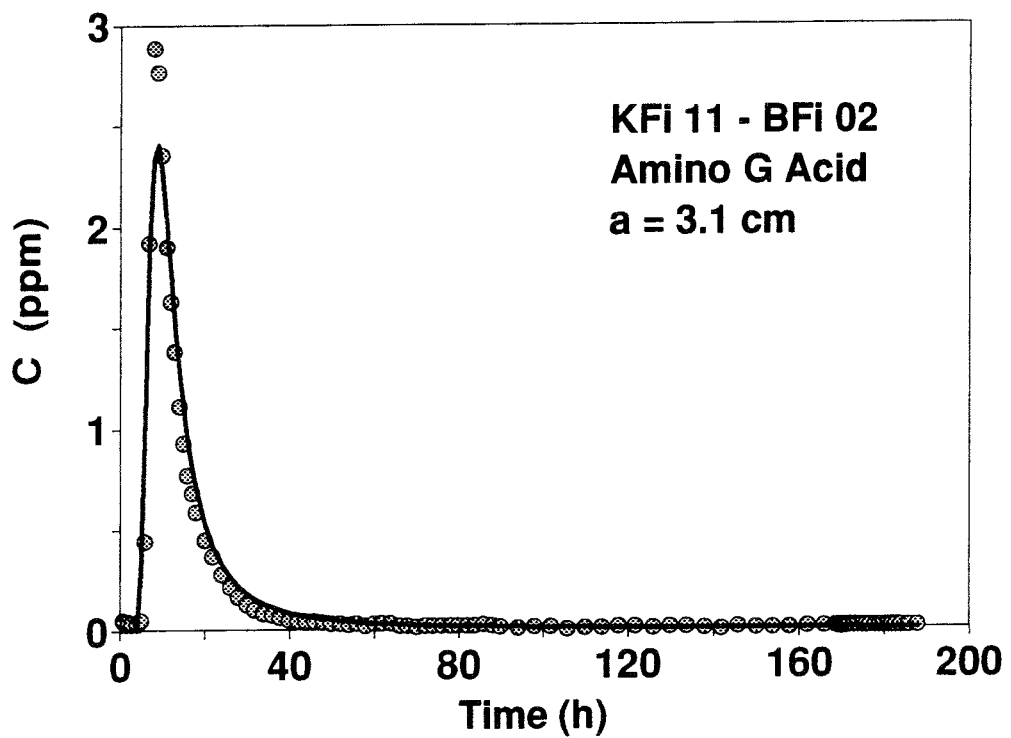


Figure 3-7. Observed and simulated (solid line) tracer breakthrough from injection in KFI11 during the preliminary tracer test. /Hautojärvi, 1993/.



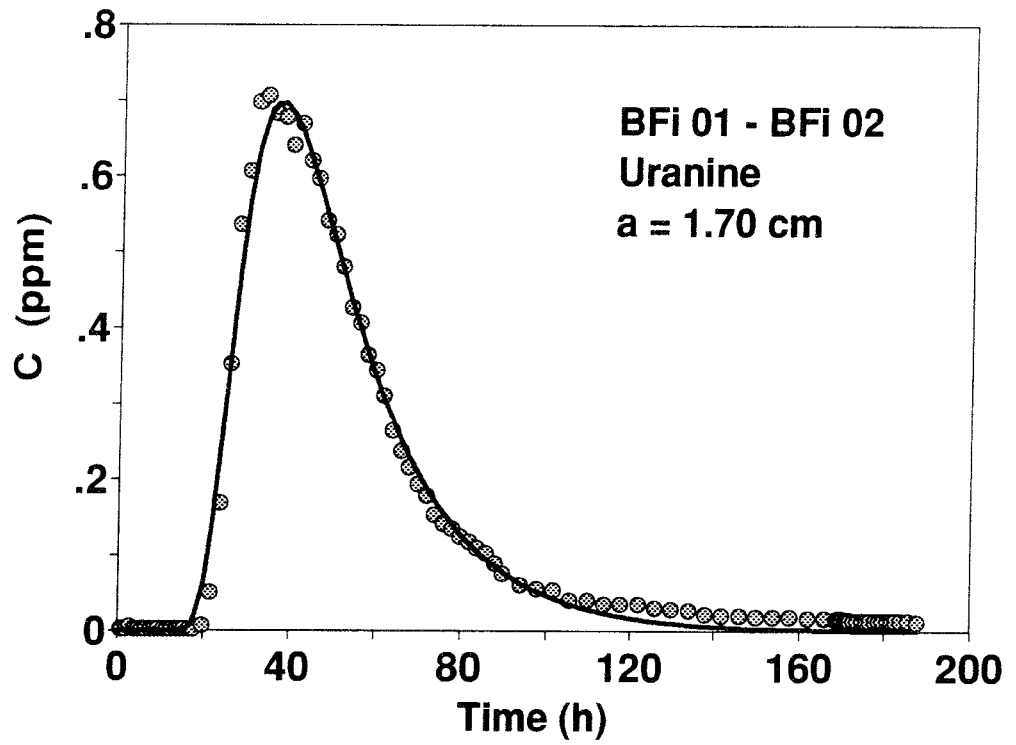


Figure 3-8. Observed and simulated (solid line) tracer breakthrough from injection in BFI01 during the preliminary tracer test. /Hautojärvi, 1993/.

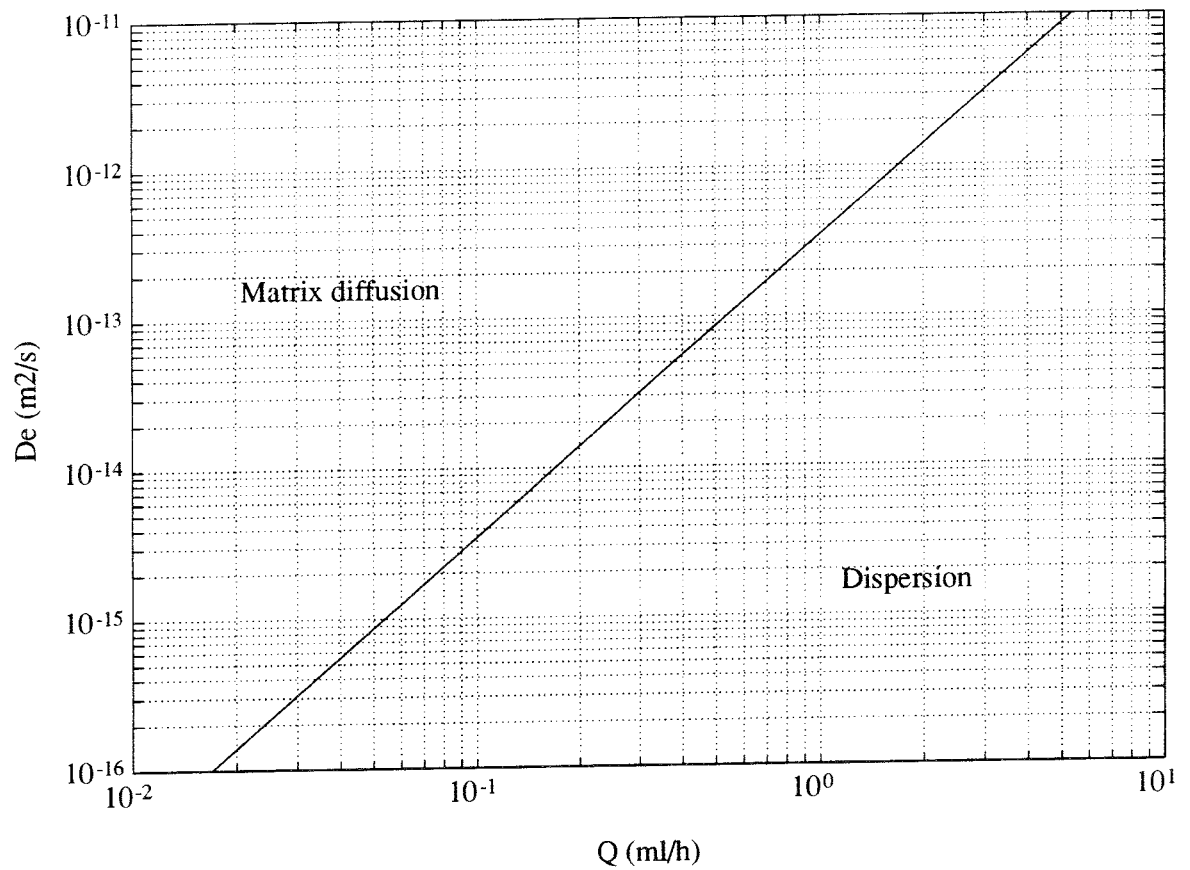


Figure 3-9. Relation between  $Q$  and  $D_e$  defining areas where hydrodynamic dispersion or matrix diffusion dominates. The following parameters are assumed: travel distance=200 m, mean velocity=0.2 m/h, channel width=0.1 m, matrix porosity=0.005 /Hautojärvi, 1992/.

### 3.3 SUMMARY OF PNC ANALYSIS

#### 3.3.1 Modelling Objectives

The main objective of the PNC analysis was to study the effect of heterogeneity on tracer transport. For that purpose a mathematical model was constructed which also enabled determination of transport parameters. The validity of the model was examined by simulation of the tracer tests performed within Zone 2 at Finnsjön.

#### 3.3.2 Modelling Approach

The basic concept of the PNC analysis was to generate a hydraulic conductivity distribution which should reflect the heterogeneous nature of Zone 2. This was done in two different ways. In the first analysis the hydraulic conductivity distribution was determined by a trial and error approach based on the measured hydraulic conductivities /Hatanaka & Mukai, 1993a/. In the second analysis the hydraulic conductivity distribution was determined using a geostatistical approach. In this analysis single-hole hydraulic test data from all eight boreholes in Zone 2 was utilized /Hatanaka & Mukai, 1993b/. Variograms were calculated and a krieged hydraulic conductivity distribution was obtained. Conditional simulations were then performed.

A porous medium, dual porosity system composed of high conductive and low conductive zones was assumed for both analyses, see Figure 3-10. In the first analysis transport was simulated using a stream tube concept and in the second analysis a two-dimensional finite difference method was used. In the high conductive zone, a one-dimensional advection-dispersion transport was considered whereas a two-dimensional situation with transverse dispersion was considered for the low-conductive zone.

The analysis was made by fitting transport parameters to the dipole experiment and then checking the validity of the model by simulation of the radially converging tracer test.

#### 3.3.3 Results

The fitting show a reasonably good agreement for all tracers except Iodide where the model seem to be unable to reproduce the tail of the breakthrough curve. Two parameters were fitted for the high conductive zone, advective porosity  $\phi_{wf}$ , and a lumped parameter  $(\phi_{df}/\phi_{wf})\alpha_{Lf}$ , see Table 3-3. By assuming that the advective and dispersive porosities are the same for both low and high conductive zones a similar lumped parameter was determined for the low conductive zone.

Table 3-3. Parameters estimated from fitting of the dipole tracer test.

Tracer	$\phi_{wf}$	$(\phi_{df}/\phi_{wf})\alpha_{Lf}$	$\phi_{wp}$	$(\phi_{dp}/\phi_{wp})\alpha_{Lp}$
In-EDTA	$8.5 \times 10^{-4}$	20	$8.5 \times 10^{-4}$	50
Tm-EDTA	$8.5 \times 10^{-4}$	10	$8.5 \times 10^{-4}$	20
Gd-DTPA	$8.5 \times 10^{-4}$	12	$8.5 \times 10^{-4}$	30
I <sup>-</sup>	$8.5 \times 10^{-4}$	2	$8.5 \times 10^{-4}$	1

$\phi_{wf}$ ,  $\phi_{wp}$  = advective porosity for high and low conductive zone, respectively  
 $\phi_{df}$ ,  $\phi_{dp}$  = diffusive porosity for high and low conductive zone, respectively  
 $\alpha_{Lf}$ ,  $\alpha_{Lp}$  = dispersivity for high and low conductive zone (m), respectively

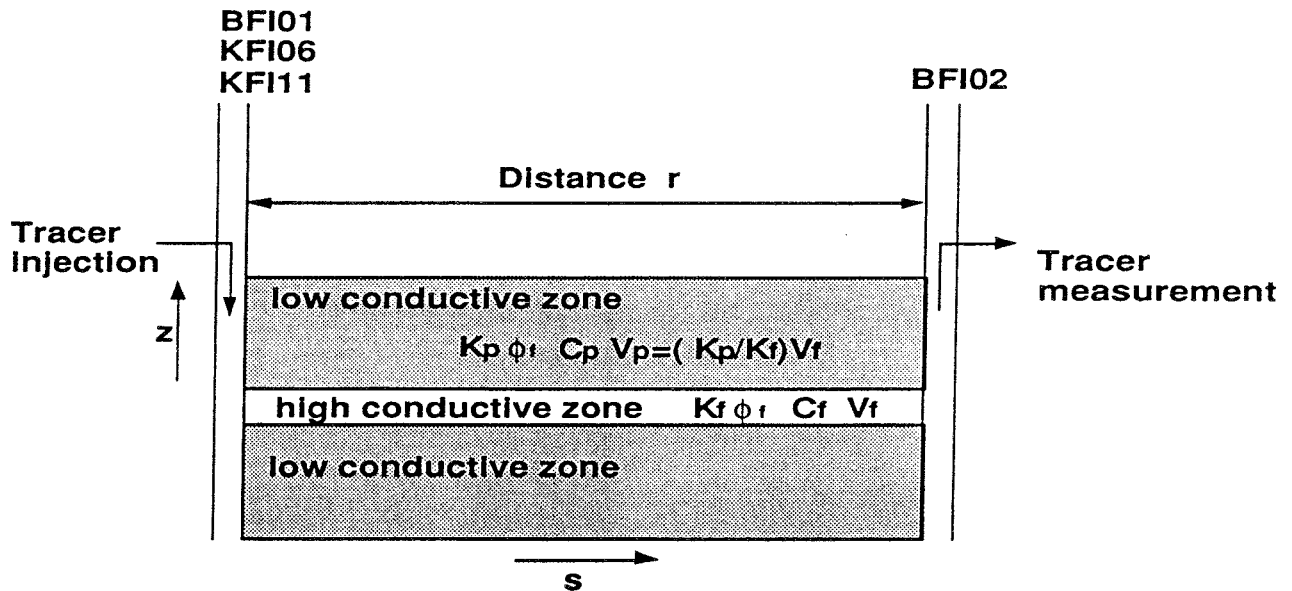
Using the parameters in Table 3-3 breakthrough curves from the three boreholes used in the radially converging test were simulated. The results show a reasonably good fit to the experimental data in the early, rising part of the breakthrough curves whereas the fitting of the tail is somewhat poorer. An example for In-EDTA is presented in Figure 3-11.

In order to improve the fit of the tail, a new set of parameters which are independent of the dipole test were assigned, and a better fit of the tails were obtained, see Figure 3-12.

### 3.3.4

#### **Conclusions**

Based on the results of their analysis the PNC team concludes that transport during both the dipole test and the radially converging test can be explained by the porous medium, double porosity model used. The dipole test breakthrough curves could be satisfactorily explained and the radially converging test could be reasonably well simulated. However, the Iodide breakthrough curve could not be well simulated under the parameter constraints. The fit leads to inconsistent parameter values.



- $K_f$  : Hydraulic conductivity of high conductive zone  
 $K_p$  : Hydraulic conductivity of low conductive zone  
 $V_f$  : Average velocity in high conductive zone  
 $V_p$  : Average velocity in low conductive zone  
 $C_f$  : Tracer concentration in high conductive zone  
 $C_p$  : Tracer concentration in low conductive zone  
 $\phi_f$  : Porosity of high conductive zone  
 $\phi_p$  : Porosity of low conductive zone

Figure 3-10. Sectional view of the fracture zone along each streamline /Hatanaka & Mukai, 1993a/.

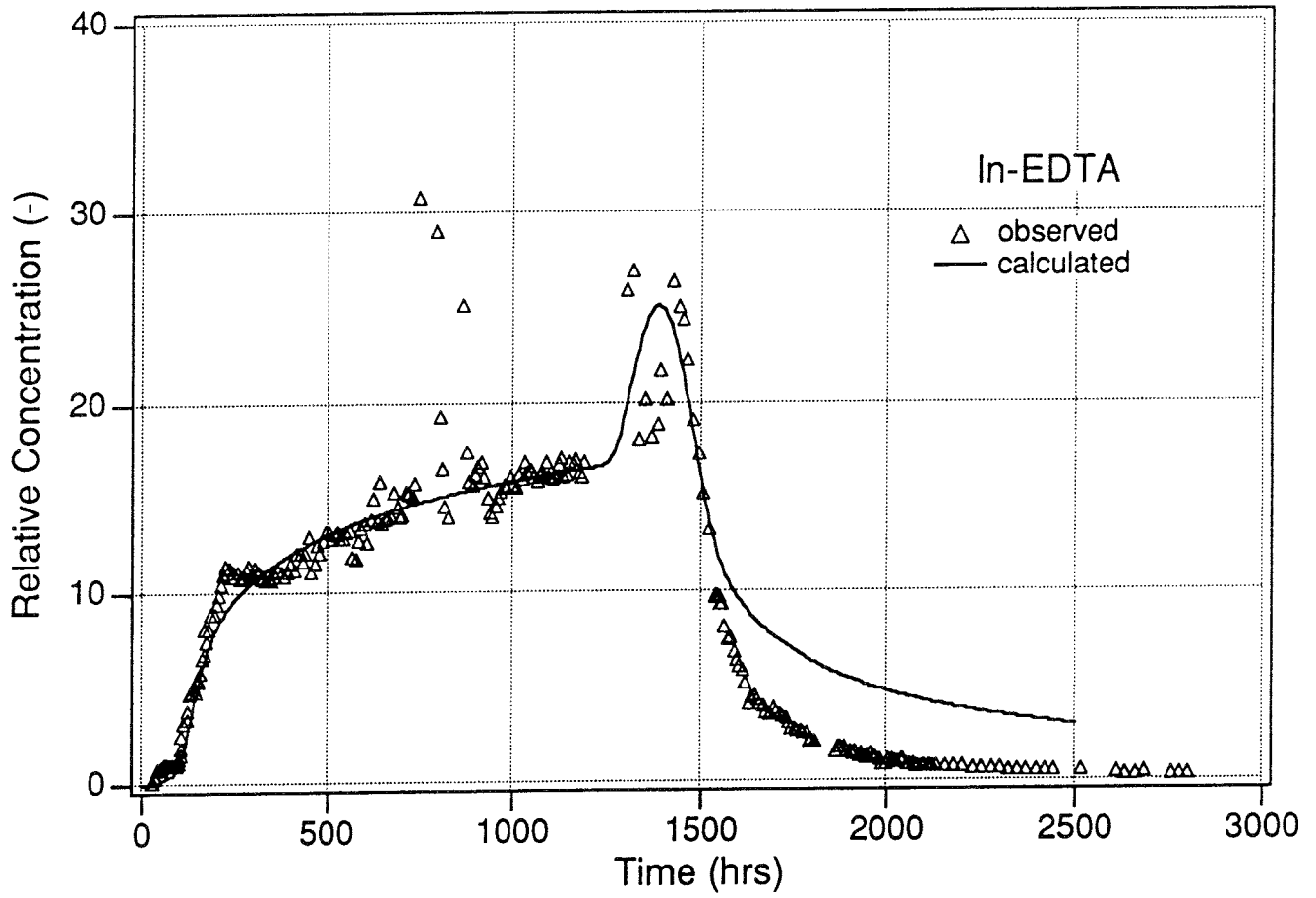


Figure 3-11. Comparison between simulations and experimental data for In-EDTA in the radially converging test based on dipole data /Hatanaka & Mukai, 1993a/.

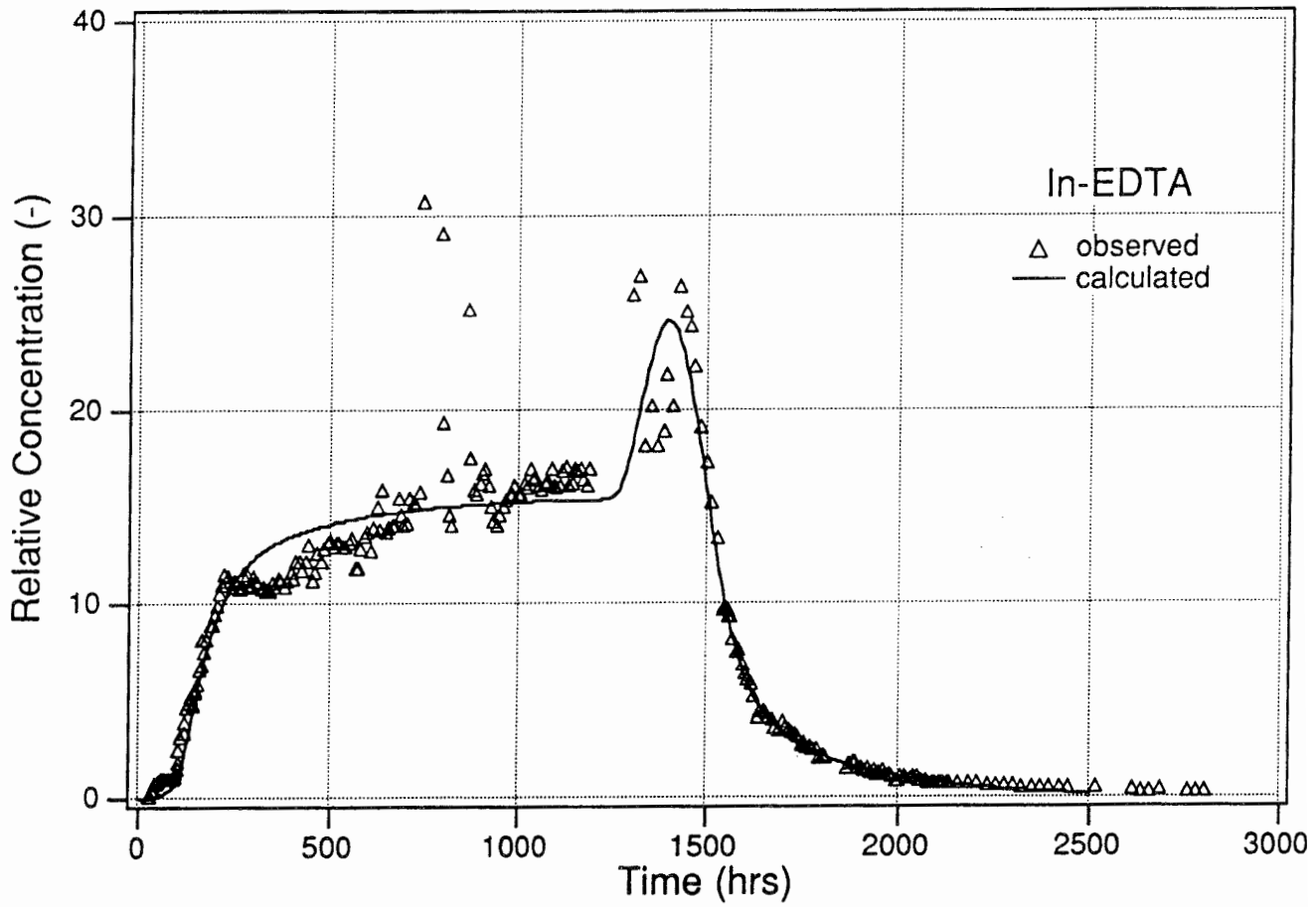


Figure 3-12. Comparison between simulations and experimental data for In-EDTA in the radially converging test based on revised set of parameters /Hatanaka & Mukai, 1993a/.

### 3.4 SUMMARY OF THE PSI/NAGRA ANALYSES

The modelling performed by the PSI/NAGRA team differs from the other INTRAVAL contributions by their use of tracer test data from another part of the Finnsjön site. The analysis is based on a series of radially converging tracer tests, using both non-sorbing and sorbing tracers, performed in 1979–82 in a minor fracture zone about 1 km south of the Brändan area /Gustafsson & Klockars, 1981, 1984/. These test have earlier been used as a test case for the INTRACOIN study /SKI, 1986/. The modelling is presented in more detail by Jakob & Hadermann (1993).

#### 3.4.1 **Modelling Objectives**

The main objective of the PSI/NAGRA analyses was to investigate if their relatively simple model could explain tracer transport at Finnsjön or, if not, what criteria could be found for a rejection of the model. Additional objectives were:

- to determine the geometrical assumptions needed to reproduce the breakthrough curves,
- to determine the dominant transport processes in the Finnsjön experiments,
- to assess if conclusions are consistent with physical comprehension of transport processes,
- to study the effects of varying flow boundaries on parameter values (both source term and downstream flow),
- to examine if extracted parameter values match those derived from independent experiments, in particular values determined during the INTRACOIN study.
- to find geometrical criteria to choose a unique set of best-fit parameter values for the non-sorbing tracer and then fix these data to determine additional transport parameter for sorbing tracers.

#### 3.4.2 **Modelling Approach**

The model is based on the assumption that the migration zone may be seen as a part of a larger planar fracture with very flat hydraulic potential. The fracture is represented by a 2D-aquifer of constant values whereas the potential corresponds to that of an unperturbed dipole field.

Tracer transport is simulated in a dual porosity system where both fracture and vein geometries for preferential flow paths are considered. Diffusion of



tracer into stagnant pore water is also considered. Sorption of the tracer on fracture/vein surfaces and onto inner surfaces of the rock matrix is described by Freundlich isotherms. Both linear and non-linear isotherms are used.

Special emphasis was put on determining the uniqueness of the model fits using the Marquardt-Levenberg method. Thus, regression parameters, their standard deviations and the corresponding correlation was determined.

The modelling was done in a stepwise manner starting with simulations of the tracer breakthrough for a non-sorbing tracer (Iodide). The simulations aimed to investigate i) the effects of variable flow boundaries, ii) influences of one or more preferential flow paths, and iii) influence of flow path geometry (fractures or veins). The intention was to find geometrical criteria to choose a unique set of best-fit parameter values for the non-sorbing tracer and then fix these data to determine additional transport parameter for the sorbing tracers (Strontium and Cesium).

### 3.4.3 **Results**

The results of a varying source term is clearly visible in the experimental breakthrough data. The modelling performed including all available information on both upstream (source term) and downstream boundaries has a clear influence on extracted best-fit parameter values. Jakob and Hadermann (1993) also found that the experimental data were too rudimentary for modelling successfully the finer details of the breakthrough curves, especially the main peak at 180–250 hours, see Figure 3–13. Matrix diffusion was found to play a minor role as transport mechanism.

The influence of one or two preferential flow paths was found to be significant. A two path system gave much better fits to the experimental data. Also, without introducing a second flow path longitudinal dispersivities ranged between 1/3 to 2/3 of the migration distance which is so large that the advection/dispersion equation may be questioned. In the two path case values scatter in the range 0.5–7.5 m or 1/60 to 1/4 of the migration distance.

The uniqueness of the obtained transport parameters was checked by repeating the calculations for the same breakthrough curve up to 30 times with different sets of starting values. The resulting best-fit parameters were found not to be unique, though agreeing within 16 error limits, when two flow paths were introduced. This loss of uniqueness was used as a reason for not introducing more than two flow paths to the system.

The influence of flow path geometry was investigated by applying a vein flow geometry instead of a fracture flow. The vein flow assumption did not yield better fits to the experimental data and was therefore not considered to be more appropriate to use.

The transport of sorbing tracers was modelled by fixing the values for the hydraulic parameters and the effective diffusivities for the non-sorbing

tracers followed by adjustment of the transport parameters for sorbing tracers, retardation factor  $R_r$ , equilibrium coefficient  $K_d$ , and Freundlich parameters. The results for the modelling of the Strontium breakthrough gives good fits assuming a two path model both with and without matrix diffusion. However, including matrix diffusion improves the regression statistics, see also Figure 3–14. Extracted best fit values for the effective diffusion coefficient are in the order of  $10^{-13}$  m<sup>2</sup>/s. The modelling also showed that it was necessary to account for tracer losses due to precipitation. Thermodynamic calculations supported this assumption.

The modelling of the Cesium transport showed that it was impossible to obtain a reasonable fit to the breakthrough curve assuming a linear sorption isotherm. Only by including non-linear sorption, reasonable fits were obtained, see Figure 3–15. The resulting Freundlich parameters were found to be compatible with literature data.

#### 3.4.4 Conclusions

Based on their analysis Jakob & Hadermann (1993) conclude:

- The experimental data available for modelling work were not sufficient to describe the breakthrough curves in every detail.
- Models with only one flow path do not satisfactory reproduce the breakthrough curves. Introducing a second flow path clearly improves the fits but this also leads to an increased number of free parameters and a loss of uniqueness of the fits.
- The breakthrough curves are better reproduced assuming fracture flow than vein flow.
- Transport is clearly dominated by advection. Matrix diffusion only has a small but non-negligible effect. Fits were improved by including matrix diffusion. Values of effective diffusivity were found to be consistent with literature data.
- The procedure of fixing values of hydraulic parameters and effective diffusivities with Iodide and then adjust sorption parameters for Strontium and Cesium was found to be successful.
- Strontium is only slightly retarded.  $K_d$  values are consistent with laboratory data. Tracer losses due to other mechanisms need to be accounted for.
- Cesium breakthrough cannot be fitted with linear sorption isotherm. Non-linear sorption is needed. Freundlich parameters are consistent with literature data.

Finally, Jakob & Hadermann (1993) conclude that the concept of a dual porosity medium has proved to be a versatile, efficient, and highly appropri-

ate concept for analyzing these migration experiments. The modelling of the Finnsjön experiments did not reach any serious limitations for the model and no other mechanism than those already incorporated in the model, had to be advocated.

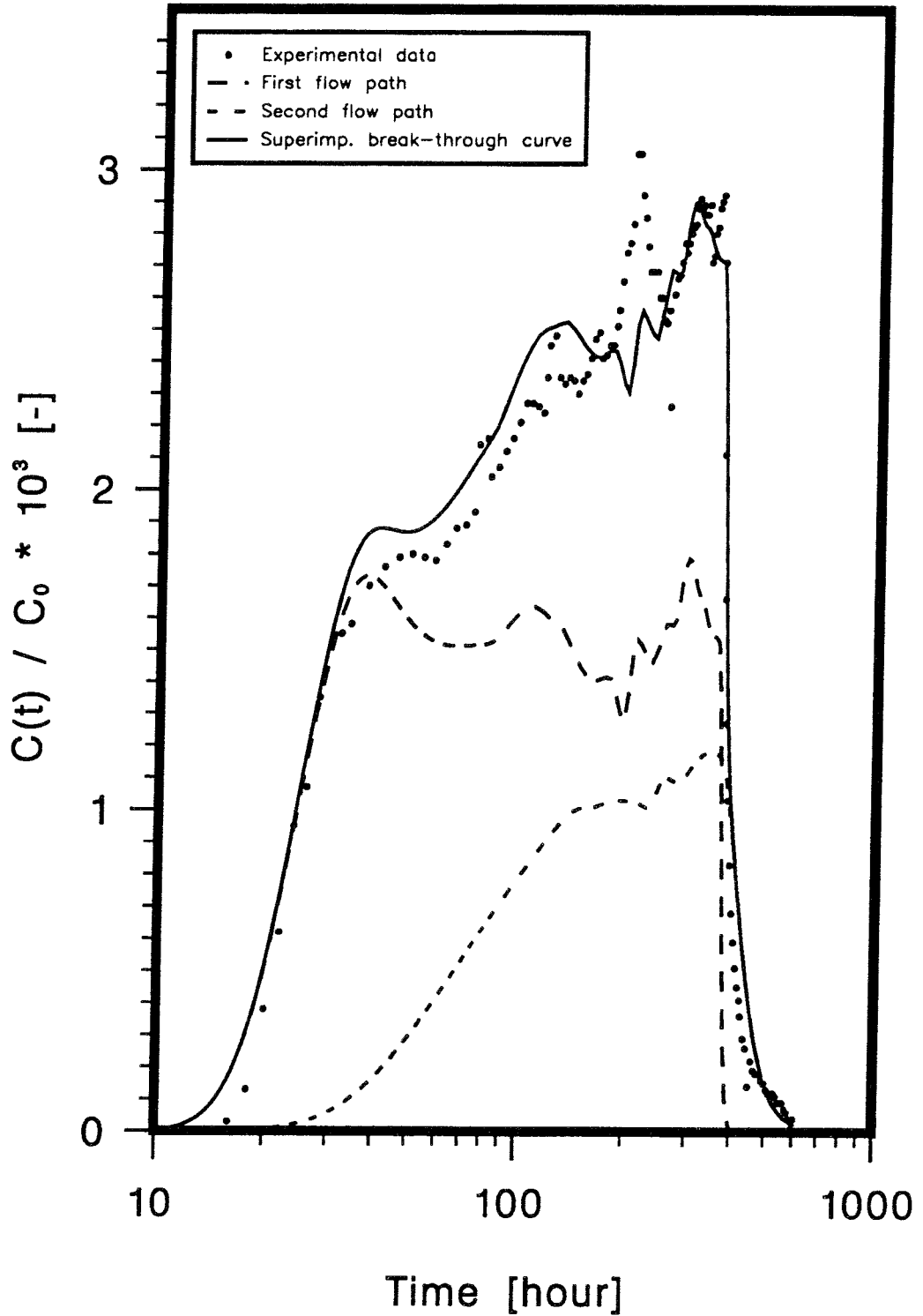


Figure 3-13. Simulation of Iodide breakthrough for a two path system including all recorded variations of upstream and downstream boundaries /Jakob & Hadermann, 1993/.

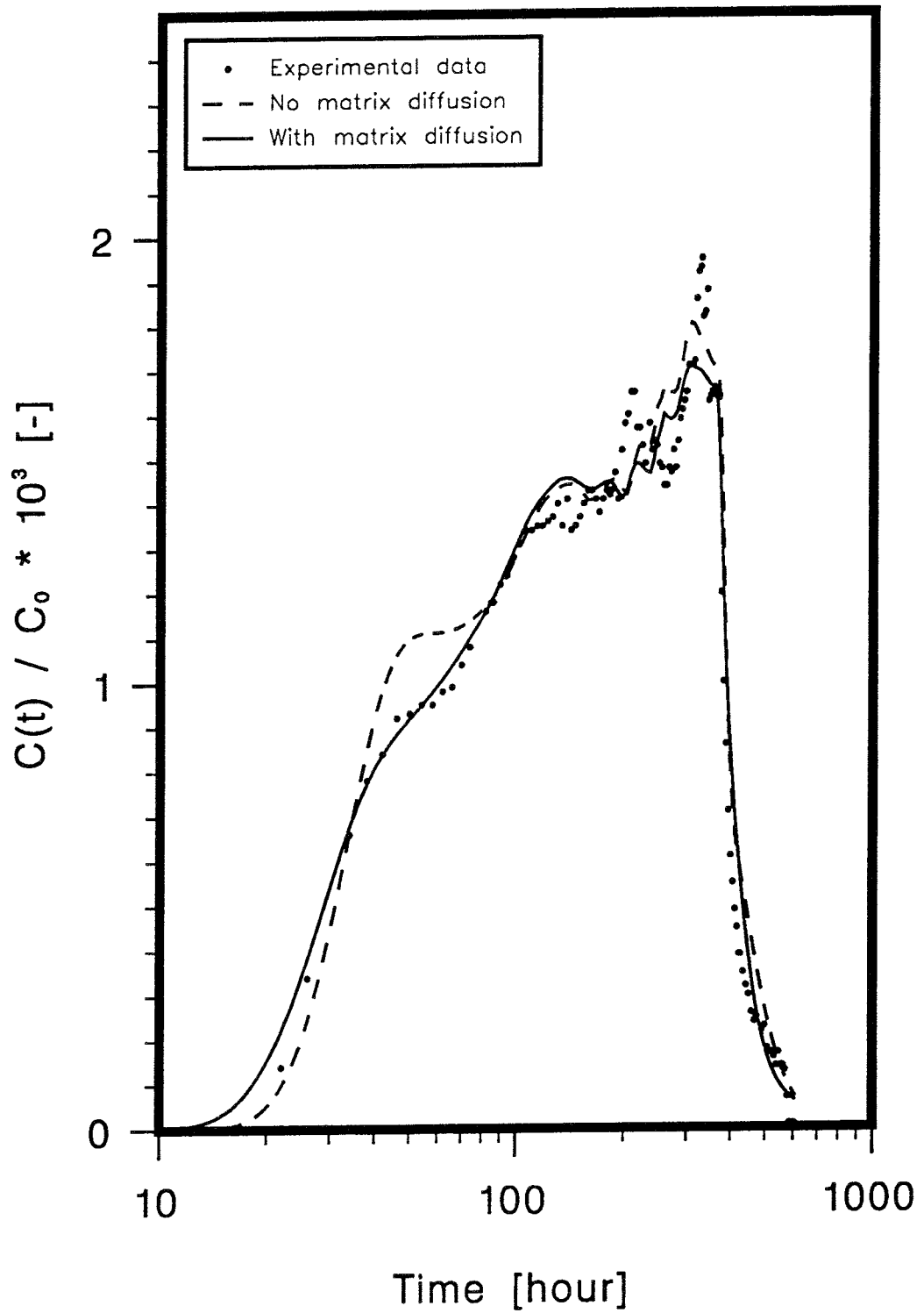


Figure 3-14. Best-fit curve and experimental data for Strontium with and without matrix diffusion /Jakob & Hadermann, 1993/.

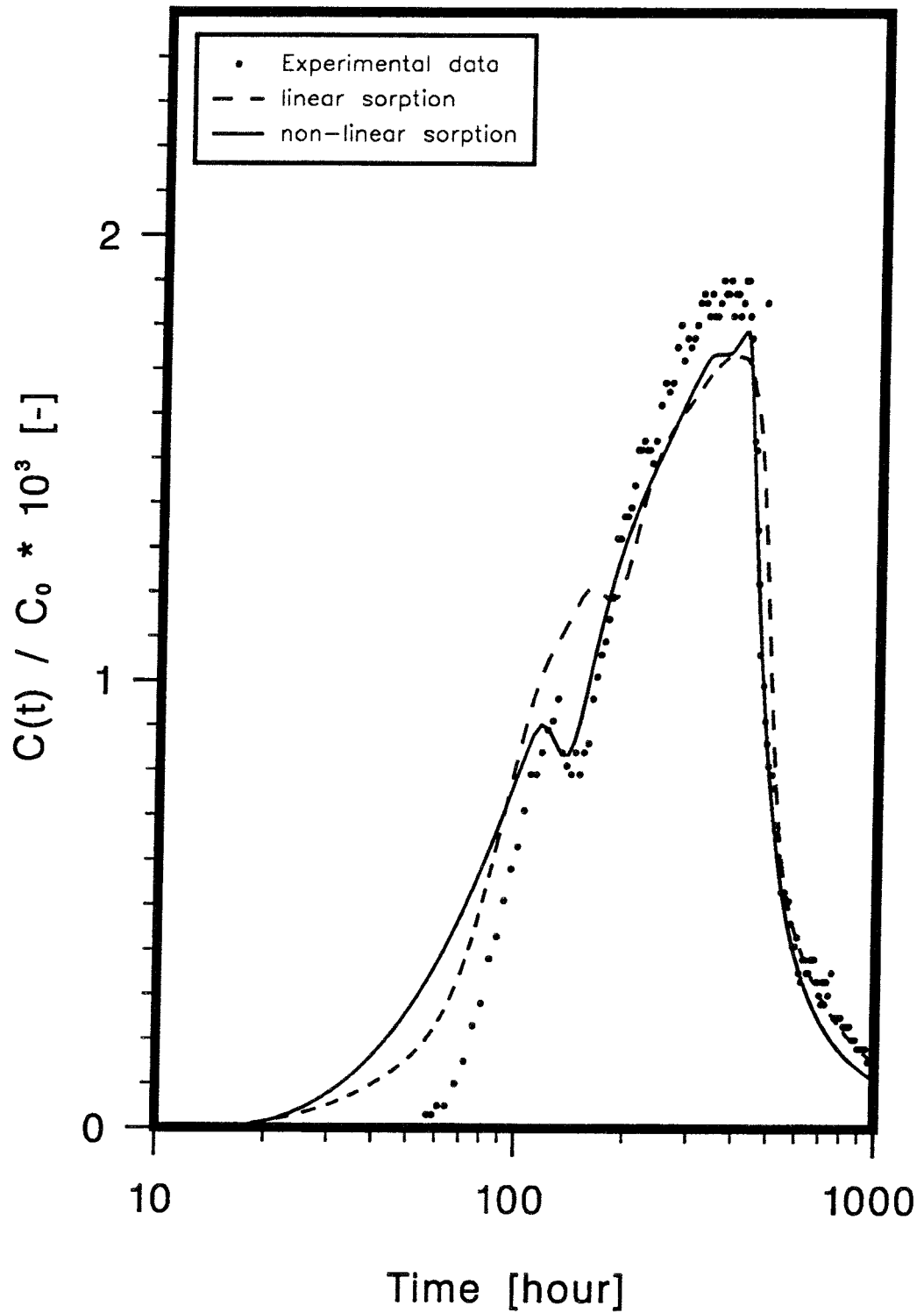


Figure 3-15. Best fit curve and experimental data for Cesium with linear and non-linear sorption isotherms /Jakob & Hadermann, 1993/.

## 3.5 SUMMARY OF THE UNIVERSITY OF NEW MEXICO ANALYSIS

### 3.5.1 **Modelling Objectives**

The objective of the UNM analysis was to investigate whether a relatively simple porous medium, single porosity model could describe the transport in Zone 2 during the radially converging experiment. Analysis of the dipole tracer test results was performed in order to validate the model. A double porosity model was also used for comparison.

### 3.5.2 **Modelling Approach**

Zone 2 and the surrounding bedrock were modelled with 2-D single porosity and double porosity models. In the system, three vertical cross-sections were used to represent the flow paths between each of the three injection holes (BFI01, KFI06, KFI11) and the pumping hole (BFI02), see Figure 3-16. Thickness and hydraulic conductivity was interpreted from the individual borehole data. In the analysis the injection wells and the pumping well were located at the boundaries. No flow boundary was assigned to the pumping well and a Dirichlet type boundary was assigned to the injection well. The flow velocity during the radially converging test was used instead of head distribution and pumping rates and only transport calculations were performed. In the single porosity model, a constant injection rate was assigned while the concentration time history was specified in the double porosity model.

About 4000 elements were used to model the entire Zone 2 with the finite difference code TRACR3D /Travis & Birdsell, 1991/.

### 3.5.3 **Results**

#### *Single porosity model*

The transport simulations were performed for 8 of the total 12 tracer injections performed during the radially converging experiment. The results show a reasonably good agreement with observed data for most of the tracers/flow paths, e.g. Uranine (Figure 3-17) while some are somewhat less good, e.g. Dy-EDTA (Figure 3-18). Ng & Kota (1993) indicate that the poor fits may be due to poor recovery or a more complex flow pattern than described in the model. The best fit parameters, porosity ( $\epsilon$ ), longitudinal dispersivity ( $\alpha_L$ ), and flow field velocity ( $u$ ), determined are given in Table 3-4. The fitting procedure resulted in longitudinal dispersivities from 10.7 to 13% ( $\alpha_L/\alpha_T = 100$ ) of the travel distance, porosities in the range of 2-10%, and velocities within a factor of 0.3 to 4.5 of the measured velocity.

Table 3-4. Best-fit parameters for the single-porosity model.

Borehole (section)	$\epsilon$	$\alpha_L$ (m)	$u$ ( $10^{-4}$ cm/s)
BFI01:U	.10*	20	7.0
BFI01:M	.035	18	0.90
BFI01:L	.05	25	0.60
KFI06:M	.046	21	0.90
KFI06:L	.02	25	1.7
KFI11:U	.04	13.5	6.0
KFI11:M	.10*	20	0.095
KFI11:L	.02	60*	0.39

\* Values out of the experimental range.

#### *Double porosity model*

The results of the fits with the double porosity model are similar to the results using the single porosity model. Most of the breakthrough curves can be fitted reasonably well with the exception of Er-EDTA and Dy-EDTA where the fits are poorer, examples are shown in Figures 3-19 and 3-20. The best fit parameters fracture aperture (2b), porosity ( $\epsilon$ ), constrictivity ( $\tau_c$ ), diffusion coefficient ( $D_i$ ), longitudinal dispersivity ( $\alpha_L$ ), and flow field velocity ( $u$ ) are summarized in Table 3-5. The fitting procedure resulted in longitudinal dispersivities from 4.2 to 13% of the travel distance, fracture apertures around 0.01 cm, matrix porosity in the range of 6.9-15%, and constrictivity of 0.155 to 0.5.

The ratios of matrix to fracture porosity, calculated based on the best-fit values, are in the order of  $10^{-2}$ , which suggests that matrix diffusion is an important process at Finnsjön /Ng & Kota, 1993/. However, no significant improvement of the fits was found in using the double porosity model compared to the single porosity model although a slightly better fit for the tail of the breakthrough curves was achieved.

Table 3-5. Best-fit parameters for the double porosity model.

Borehole (section)	2b (cm)	$\epsilon$	$\tau_c$	$D_i$ ( $\text{cm}^2/\text{s}$ )	$\alpha_L$ (m)	$u$ ( $10^{-3}$ cm/s)
BFI01:U	.011	.095	.39	$10^{-5}$	20	4.55
BFI01:M	.010	.11	.255	$10^{-5}$	20	1.75
BFI01:L	.010	.10	.155	$10^{-5}$	8.5	1.2
KFI06:M	.010	.069	.25	$10^{-5}$	18	1.23
KFI06:L	.010	.15	.48	$10^{-5}$	18	2.7
KFI11:U	.010	.101	.50	$10^{-5}$	18	5
KFI11:M	.010	.105	.39	$10^{-5}$	22	9.7
KFI11:L	.010	.15	.49	$10^{-5}$	15	2.35

### *Dipole tracer test*

The analysis of the dipole test was mainly carried out to validate the models used to interpret the radially converging test. So far, only the single porosity model has been used. The analysis was performed by assigning the best fit parameters determined from the radially converging test to the upper, 5 m layer, of Zone 2 and using the dipole flow velocity and tracer injection data. The agreement between the simulated and observed data was found to be good (Figure 3–21) and Ng & Kota (1993) finds it reasonable to say that the single porosity model is validated.

### *Sensitivity analysis*

Ng & Kota (1993) also performed a sensitivity analysis of both models. In both models peak concentrations were found to be sensitive to changes in any of the parameters. The most sensitive parameter was found to be longitudinal dispersivity ( $\alpha_L$ ). Arrival times were found to be sensitive only to changes in porosity ( $\epsilon$ ) and flow velocity ( $u$ ) in the single porosity model and to longitudinal dispersivity ( $\alpha_L$ ) in the double porosity model.

## 3.5.4

### **Conclusions**

A comparison of the results of the single and double porosity models shows that both models display reasonable agreement with the observed breakthrough curves except in the cases of KFI11:M and KFI11:L, where neither model can reproduce the breakthrough curves. Low recovery of these two tracers may be the reason. The two models yield similar regression coefficients ( $r^2$ ) and it cannot be judged which model is best representing Zone 2. However, based on the validation of the single porosity model using the dipole test analysis, such a model can be used for Zone 2.

Ng & Kota (1993) also concludes that the interpreted results of the tracer tests strongly depend on the model used. This implies that properties of the medium (e.g. porosity and longitudinal dispersivity) calculated from the two models, are determined by the processes which are included in a certain model. Finally, a three-dimensional analysis is suggested in order to gain a better insight of the transport mechanisms in Zone 2.



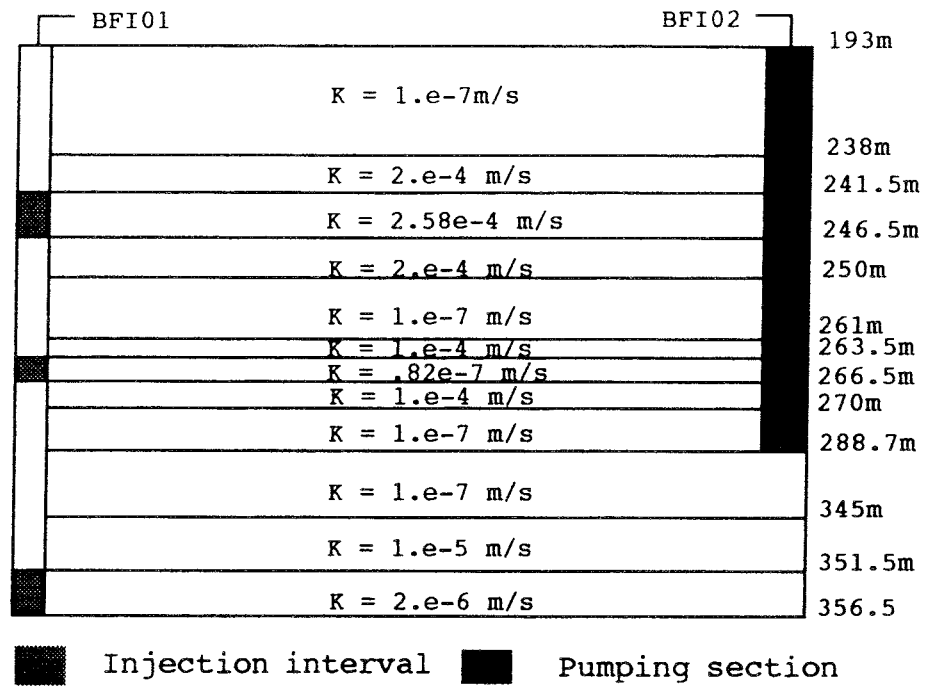


Figure 3-16. Distribution of layers and parameter values in cross-section BFI01-BFI02 /Ng & Kota, 1993/.

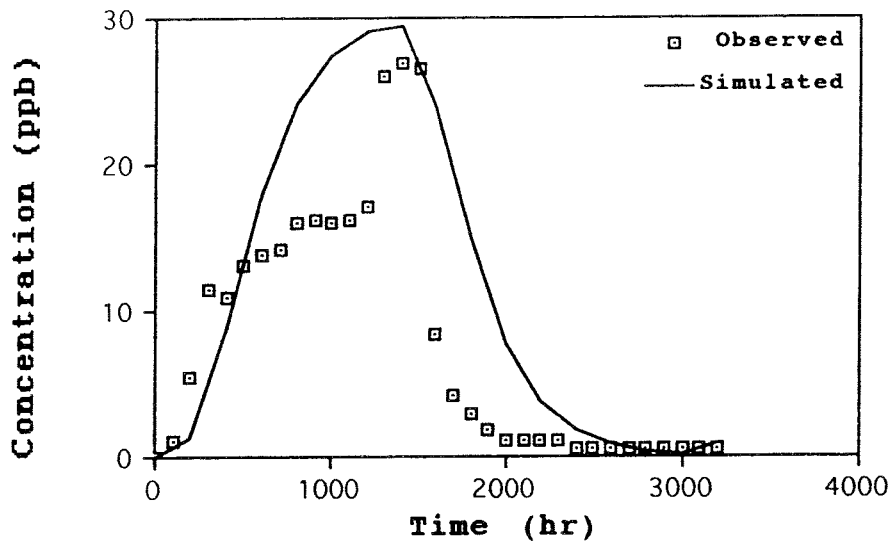


Figure 3-17. Comparison between simulation with the single porosity model and observed breakthrough data for In-EDTA (BFI01:U) /Ng & Kota, 1993/.

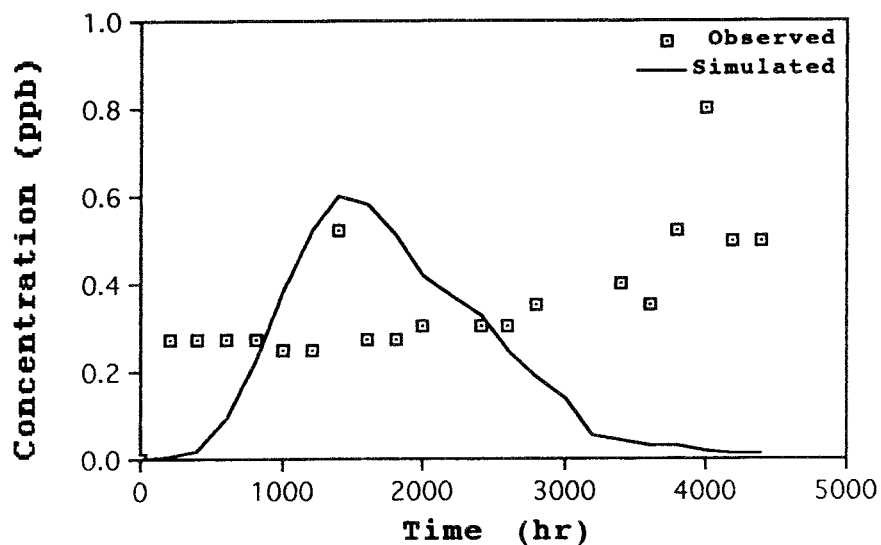


Figure 3-18. Comparison between simulation with the single porosity model and observed breakthrough data for Dy-EDTA (KF111:L) /Ng & Kota, 1993/.

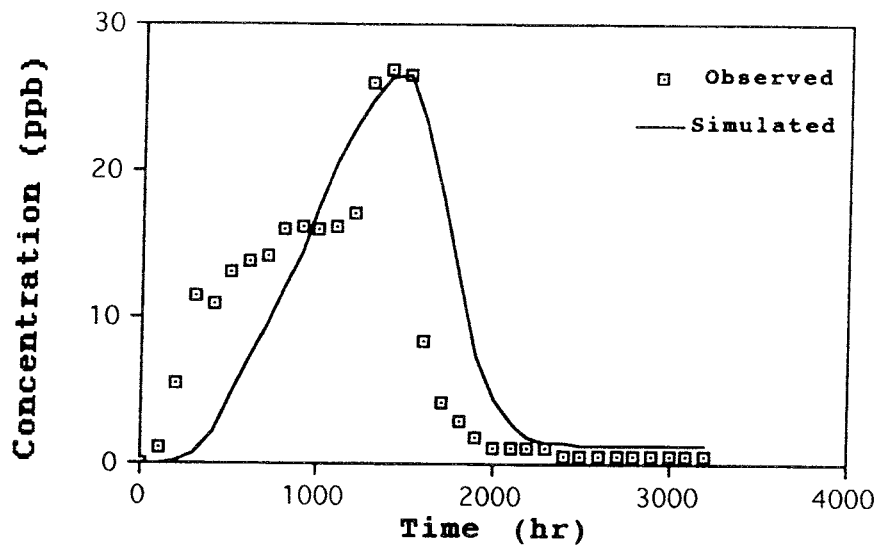


Figure 3-19. Comparison between simulation with the double porosity model and observed breakthrough data for In-EDTA (BFI01:U) /Ng & Kota, 1993/.

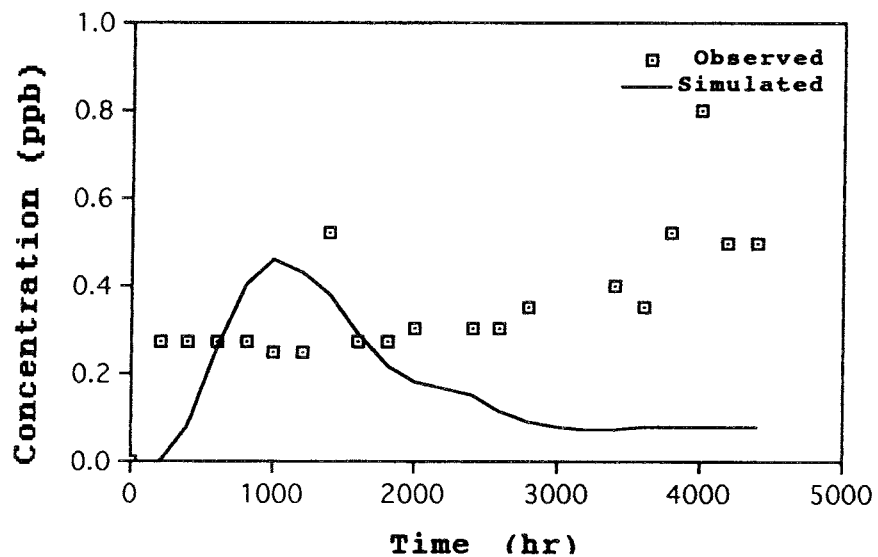


Figure 3-20. Comparison between simulation with the double porosity model and observed breakthrough data for Dy-EDTA (KFI11:L) /Ng & Kota, 1993/.

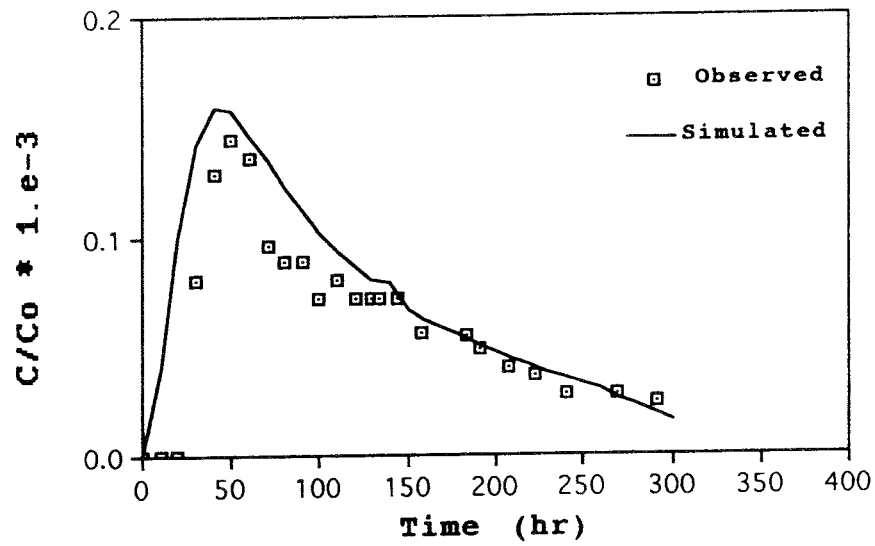


Figure 3-21. Comparison between simulation of the dipole test with the single porosity model and observed breakthrough data for In-EDTA (BFI01:U) /Ng & Kota, 1993/.

## 3.6 SUMMARY OF HAZAMA CORPORATION ANALYSIS

### 3.6.1 Modelling Objectives

The Hazama analysis within Phase 2 includes flow and transport analysis of the radially converging tracer test. The objective is to address the problem using a representative elementary volume approach which also includes description of anisotropy and spatial variability in permeability /Kobayashi & Yamashita, 1993/.

### 3.6.2 Modelling Approach

The first step in the model approach is an estimation of a representative elementary volume on the basis of measured fracture density and an assumed fracture trace length. The fracture frequency ( $1/[L]$ ) of identified fracture sets is used to solve for the fracture density ( $1/[L^3]$ ) of individual fracture sets assuming three different fracture length distributions. A measure of the representative elementary volume (REV) is subsequently obtained through the Crack Tensor Theory /Oda, 1986/ using the geometry and properties of the fractures involved in the analysis. The permeability tensor  $k_{ij}$  based on single hole data and a matrix  $Q_{ij}$  which includes fracture geometrical information is used to calculate an apparent aperture  $\alpha_{ij}$  for the REV. The variogram of the three principal components of  $\alpha_{ij}$  is calculated as is that of the mean value, assumed to be a scalar.

In the subsequent numerical analysis of flow and transport, a finite element model of fracture zone 2 was devised with a size of 1000x1000x100m. A central 300x300 m area is discretized in more detail with 20x20x20 m blocks, c.f. Figure 3-22. Values of isotropic apparent aperture  $\alpha$  are assigned to the FEM model using conditional simulation. A total of 500 realizations were generated. In addition a homogeneous value of  $Q_{ij}$  was assigned to all element blocks. Prescribed head boundary conditions are assigned to all faces of the numerical model. The pumping rate applied in BFI02 to simulate the tracer test is 2 litres/s.

For the transport calculations a particle tracking procedure was used. As a first try, the porosity derived from the Crack Tensor Theory was assigned to the model. This porosity is proportional to  $\alpha$  and the fracture length squared, and is thus also heterogeneous. A particle is released from various test sections in BFI01, BFI06 and KFI11 and the tracer breakthrough curve is estimated from the ensemble of arrival times for the various realizations. The porosity is calibrated by obtaining an agreement between measured and simulated breakthrough curves.

### 3.6.3 Results

The analysis showed that the length scale of the representative elementary volume is in the order of 20m, hence the selection of the element size in the densely discretized area. The transport results are presented as figures comparing measured breakthrough with simulated results (ensemble average) for different injection points (upper (U), middle (M) and lower (L) test section in BFI01, KFI06 and KFI11, c.f. Figure 3–23. Because the tracer recovery losses are not explicitly considered in the calculations, the concentration of each particle is multiplied with the recovery rate for each injection point. The much more rapid rise in the simulated breakthrough curves indicates that the calculated velocity field is overestimated for the whole model domain, particularly so for the middle (M) and lower (L) regions.

### 3.6.4 Conclusions

The authors claim that although the approach to obtain the characteristics of the anisotropic, heterogeneous media may appear complicated and troublesome, the field data have been processed with care. They admit that there may still be many assumptions which are still unverified theoretically. In order to obtain better agreement between calculated and measured breakthrough curves it is i.e. necessary to revisit the process to infer the fracture length, its standard deviation and distribution function. It is stated that the results appear good although the assumptions regarding the latter three parameters remain unverified.

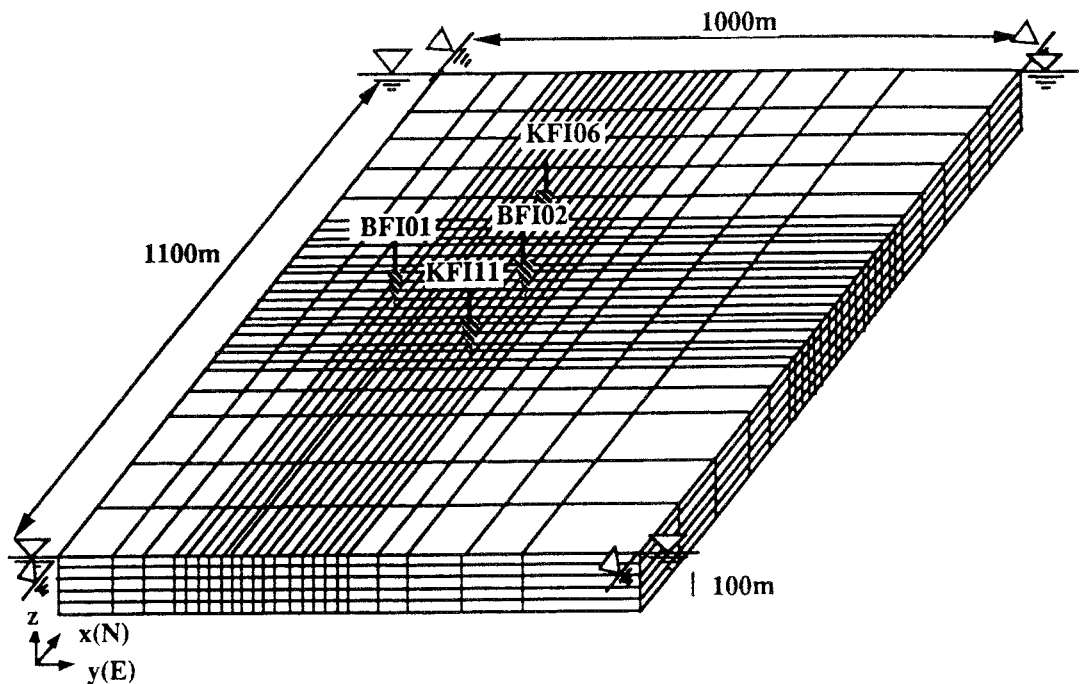


Figure 3–22. Schematic view of the finite element mesh and boundary conditions applied in the numerical analysis

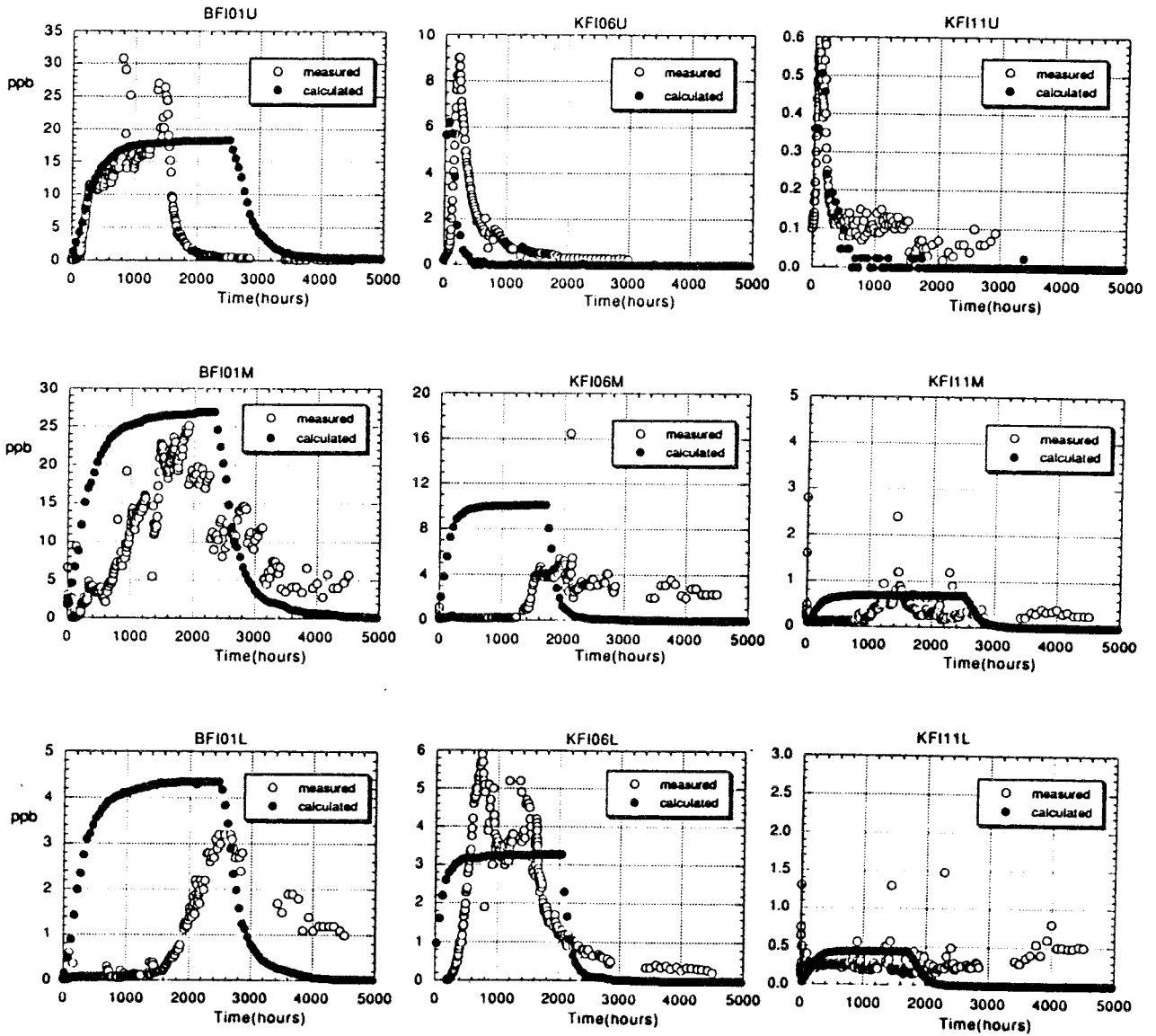


Figure 3-23. Radially converging tracer test. Comparison between measured (o) and calculated (o) breakthrough for tracer injected in different sections. Concentrations in (ppb) apart from KAS06:U (ppm).

## 3.7 CONTERRA/KTH-WRE ANALYSIS

### 3.7.1 Modelling Objectives

In most practical situations in performance assessment related studies the licensee faces the need to extrapolate a model calibrated (and possibly validated) on a local scale to a larger and more relevant transport scale. In their analysis the authors explore this problem and test whether a stochastic continuum model calibrated on a local test scale also can be validated on a larger, far-field scale (Kung et al., 1992). The analysis is performed using a model with physical conditions similar to those prevailing during the Finnsjön dipole test.

### 3.7.2 Modelling Approach

At first a reference transmissivity field was conceived over a 1200x1200 m area corresponding to the upper conductive part of Zone 2. This field was constructed through conditional parametric simulation using the turning bands method conditioned on transmissivity values from the field centred on the high-conductive part of Zone 2 in 8 boreholes. The input data which is based on the data from the 8 boreholes are assumed to be log-normal with a mean  $Y = \log_{10} K$  of  $-3.28$  ( $\log_{10}$  m/s) and a variance of  $0.15$  ( $\log_{10}$  m/s)<sup>2</sup> with an isotropic covariance structure with a 100m correlation length. The dipole tracer test was simulated in the reference field under conditions similar to the actual field conditions including a prevailing linear natural gradient of 3%. The transport simulations were performed using a particle tracking routine assuming conservative particles and only taking advection into account. The resulting breakthrough curves for tracer released in KF11 and BF101 were considered as the real system response of the reference field to be used for calibration. Subsequently, a far-field tracer experiment under natural gradient conditions was simulated by releasing tracer along the upstream boundary and monitoring of breakthrough along the downstream boundary of the model. The results of the latter experiment are to be used for validation of extrapolation to the far-field scale of a model calibrated on a local scale.

Following the analysis of the reference field, 100 equiprobable conditioned realizations were generated. The ensemble mean head distribution and the ensemble mean breakthrough for the two local scale test cases were calculated. In the subsequent calibration process only two parameters, the porosity and effective thickness of the aquifer were considered. Yet another calibration approach was utilized whereby a defined index of deviation was used to select the individual realizations which best recreated the response of the local scale tracer test. For sake of validation the far-field results of the identified realizations were compared with the reference case far-field response.



### 3.7.3 **Results**

The results showed that the ensemble mean of the calculated hydraulic head compared well with that calculated for the reference field. The transport calculations on a local scale showed that the ensemble mean breakthrough curve for the tracer release in BFI01 compared well with the reference case results, c.f. Figure 3-24. The corresponding results for tracer release in KFI11 was not as good. In this case the reference case results are not even contained within the one standard deviation envelope, c.f. Figure 3-25. The calibration based on physical parameters showed that a porosity  $n=0.025$  and an effective thickness of  $b=0.5\text{m}$  are to be used. The alternative calibration based on the index of deviation showed that three realizations best recapture the characteristics of the reference case. The far-field breakthrough curves of the particular realization with the best deviation index is shown in Figure 3-26. The results based on these realizations should be compared with the results of the far-field tracer test based on the reference field, c.f. Figure 3-27. It was found that none of the three realizations gave transport results similar to the reference case results. It can also be noted that the ensemble far-field breakthrough curve with associated uncertainty measure, c.f. Figure 3-27, does not resemble nor encompass the reference field results. The reason for the latter is the fact that there simply are not enough conditioning points on the far-field scale to recapture the characteristics of the far-field reference case transport response. A test to add 24 more conditioning points in on a far-field scale improved the results to some degree.

### 3.7.4 **Conclusions**

Two ways to calibrate a local scale model are presented, the first using the model's constant parameters, the porosity and the effective thickness, and the second being calibration to a particular field with the same output characteristics as the reference case results. The first approach showed that calibration on a local scale is insufficient to produce acceptable model predictions on a larger scale. The second approach, deterministic in nature, shows that the best fitted calibrated field(-s) on a local scale does not turn out to produce validated results on a larger scale. This shows that calibration of a model on a local scale is insufficient to also validate the model on another larger transport scale.

Calibration is better performed using statistical approaches rather than in a deterministic way. This because it is better to resort to the uncertainty measure provided by the statistical approach rather than selecting one "best fit" realization, which could also be difficult to select. Calibration and validation of stochastic continuum models still remain biased through subjectivity, but perhaps the work performed by Luis & McLaughlin (1991) and Ababou et al. (1992) may provide means to make the calibration process less subjective. Measurement data should be collected on scales relevant to the transport problem studied. A natural gradient test is regarded as a ideal validation tool but is, however in most cases practically unfeasible. An acceptable compromise may be a number of tracer tests on a smaller

scale, thus providing means for piecewise information, calibration and even validation of the performance assessment.

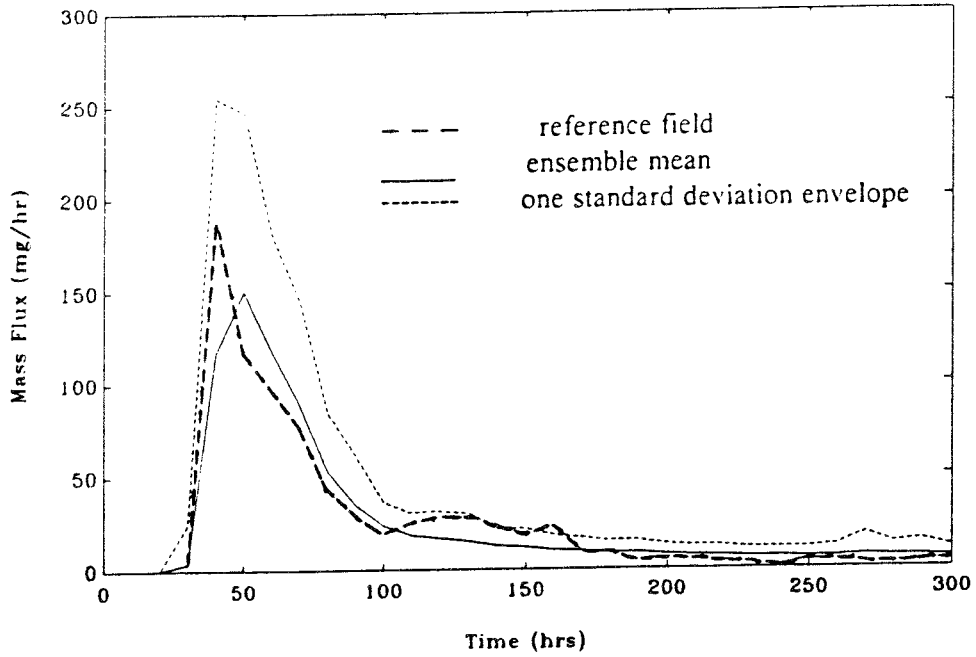


Figure 3-24. Ensemble mean breakthrough curve at BFI02, Case 1 - particles released at BFI01 (porosity  $n=0.025$ )

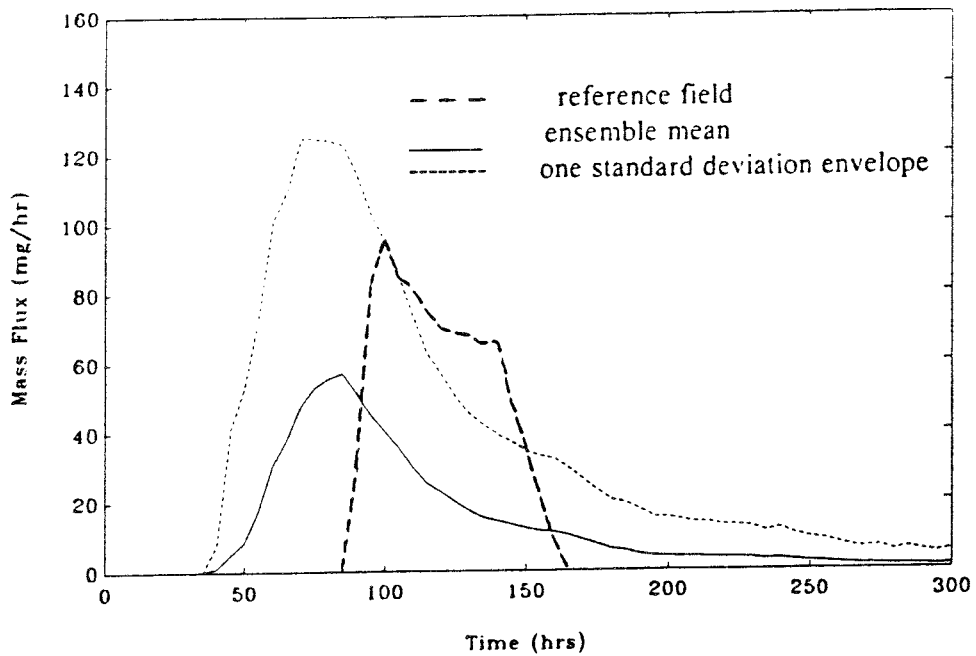


Figure 3-25. Ensemble mean breakthrough curve at BFI02, Case 2 - particles released at KFI11 (porosity  $n=0.025$ )

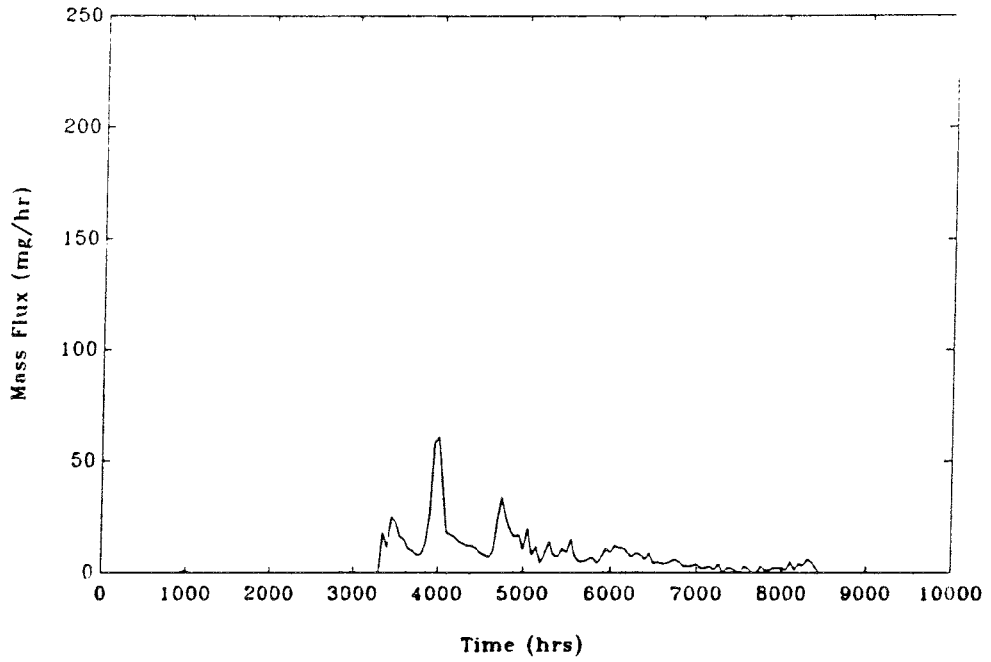


Figure 3-26 Far-field breakthrough curve for realization #22.

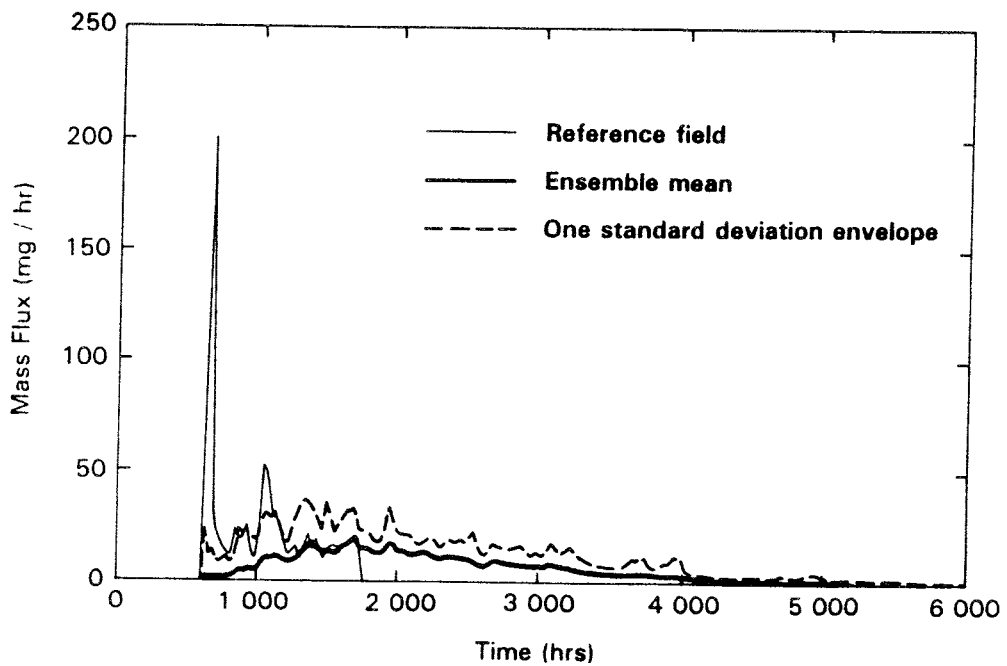


Figure 3-27. Far-field breakthrough curve for the reference field and ensemble mean breakthrough curve for the far-field simulations.

## 3.8 BRGM/ANDRA ANALYSIS

### 3.8.1 Modelling Objectives

The BRGM/ANDRA analysis has focused on the interference tests and the subsequent converging tracer test. The objectives of the analysis of the interference tests are a) to take boundary effects into account when interpreting the tests in Zone 2 using analytical techniques, b) to take the multilayering of Zone 2 into account using an axi-symmetrical finite difference model, and c) to simulate the interference tests in three dimensions. The aim in the latter case is to calibrate the model with two tests (no. 1 and 2) and to validate the model by simulating the 3A and 3B tests. The objective of the analysis of the converging tracer test are a) to interpret the breakthrough of tracers injected in the upper sections of BFI01, KFI06 and KFI11 using an analytical technique, and b) numerical modelling of the solute transport with a 3D particle tracking model focusing; i) on the four tracers injected in the upper section (DTPA, Amino-G-acid, Tm-EDTA and In-EDTA), and ii) on the tracers (i.a. Yb-EDTA) injected in the intermediate resistive layer.

### 3.8.2 Modelling Approach

In the analytical approach which addresses the effects of hydraulic boundaries, a Theis scheme accounting for boundaries was utilized /Schwartz et al., 1993/. Each of the pumping tests was considered separately. A hydraulic boundary (prescribed constant head or no-flow boundary) was considered at a specified distance  $D$  from the line joining the pump- and observation sections considered. Calibration of transmissivity  $T$ , storativity  $S$  and distance  $D$  was carried out.

The axi-symmetrical finite difference approach, which also incorporates boundary effects through "virtual" image theory, allows a simultaneous calibration of the three measurement sections for a given borehole under the assumption that the upper and lower layers have the same hydrodynamic parameters.

The numerical study in three dimensions employs a porous medium finite difference model MARTHE /Thiery 1990/ which takes the actual Zone 2 geometry and acting boundary conditions into account /Schwartz et al., 1993/. The model has a parallelogram shape with a base length of 2500m and a height of 1200 m corresponding to the model geometry employed by SKB /Andersson et al 1989/. The model consists of 5 layers, representing subzones 1 and 2, the intermediate low-permeable zone, and subzones 3 and 4, respectively. The calibration was carried out on test no. 1 and 2 using an automatic procedure which allowed determination of the best hydraulic conductivity  $K$  and specific storage  $S_s$  fields within the so-called Brändan block that minimizes a given criterion simultaneously at 300 calibration points in KFI05, KFI06, KFI09, KFI10 and KFI11. The calibrated parameter field was validated using the calibrated field to simulate and estimate the

corresponding drawdowns during tests no. 3A and 3B. Considering the different conditions employed during the calibration sequence and the validation sequence, the results could be indicative of the representability of the calibrated parameters.

The analytical approach on the converging tracer test was made using a code CATTI which includes a solution which incorporates bidimensional flow and is valid for a pulse injection in a 2D converging flow field /Schwartz, 1993/.

The premises for the numerical analysis were the hydraulic conductivity and specific storage fields calibrated/validated using the interference tests, the latter which were used to calculate the 3D Darcy velocity field. The transport simulations were made assuming continuous injection at constant rate into volumes of the model which corresponds to the actual field situation and at levels located in the middle of the corresponding layer. The calibration process was limited to a few parameters to ensure their representability. Hence, the longitudinal and transverse dispersivities  $\alpha_L$  and  $\alpha_T$  were assumed homogeneous for the whole model domain and the assigned porosities were assumed homogeneous for each simulated (test) section. Following a calibration on the tracers injected in KFI11 the obtained transport parameters were used to simulate the In-EDTA injected in borehole BFI01. Subsequently, an attempt to simulate the observed low recovery of tracers injected in the low-permeable middle section was made.

### 3.8.3

#### **Results**

The results of the analytical analysis incorporating hydraulic boundaries show a good agreement between the  $T$  and  $S$  values obtained and those presented by SKB /Andersson et al., 1989/ through analysis according to Hantush. Further analysis showed the difficulty involved in linking boundaries determined in this way with actual boundary conditions, e.g existing fracture zones and lakes, and identified the need for the three-dimensional numerical analysis. The axi-symmetric finite difference analysis yielded hydrodynamic parameters in the three layers which were consistent between boreholes, and were also in accord with those obtained through the analytical approach, and also allowed a check of the vertical flow component between neighboring layers. Similarly to the analytical approach it also suffered from limitations due to the complex fracture system which prompted for a three-dimensional description.

The results of the three-dimensional numerical analysis showed a good fit between measured and calculated drawdown during the complete test sequence for test sections in KFI05, KFI06, KFI09 and KFI10, c.f. Figure 3-28. The vertical component of the hydraulic head gradient in KFI06 was well simulated during tests no. 1 and 2. Local discrepancies may be observed at later times of the pump phase in KFI11 where the drawdown is underestimated. The "degree of fit" observed during the calibration and validation phases are very similar.

The results of the analytical analysis of the tracer test in the upper section provided first estimates of porosity  $n$  ranging from  $1 \times 10^{-4}$  to  $3 \times 10^{-4}$  depending on the tracer analyzed. The estimated longitudinal dispersivities  $\alpha_L$  range between 15 to 30 m. The results are graphically illustrated in Figure 3–29.

The analysis of tracers injected in KFI11 yielded "best" values of the transport parameters through a fitting and reduction of error procedure for all tracers concerned. The resulting set of parameters are; dispersivities  $\alpha_L = 10$  m,  $\alpha_T = 0.25$  m and a porosity  $n$  assigned to the upper test section of  $2 \times 10^{-5}$ . Figure 3–30 show a generally good fit between measured and simulated concentrations for the Gd–DTPA injected in KFI11. In order to match the In–EDTA results in BFI01 the porosity in the upper section had to be increased to  $3 \times 10^{-4}$ .

The analysis of the tracer injected into the low–permeable central section showed that the phenomenon could not be explained fully by increasing the dispersion coefficient and porosity. The authors agree with Gustafsson et al. (1990) in that chemical processes, e.g. clogging may explain the observed low recovery rates.

#### 3.8.4 Conclusions

Using a hydraulic conductivity and storativity distribution equal to that employed by SKB and further calibration and optimization of the same parameters within the Brändan block using a three–dimensional finite difference model showed that variations in drawdown could be well simulated in KFI05, KFI06, KFI09 and KFI10 during the complete interference test sequence. The same "degree of fit" was observed during the calibration and validation phase. The equivalent parameters obtained after the calibration phase are consistent with the values estimated from the 2D SUTRA and analytical Hantush analysis performed by SKB.

The analysis of the tracer test shows that it is possible to simulate the behavior of the four tracers injected in the upper conductive section. It was however noted that the differences in first arrival time for different tracers injected in the upper section makes it impossible to calibrate the model using one homogeneous porosity. Hydraulic phenomena alone are not sufficient to explain the low tracer recovery observed in the middle and lower test sections. Chemical reactions, i.a. irreversible interactions, chemical clogging in the injection sections are possible explanations for the observed phenomena. The authors identify that simulation of the Dipole Tracer experiment which was performed subsequently in the same borehole array provides a means to validate the calibrated transport parameters.

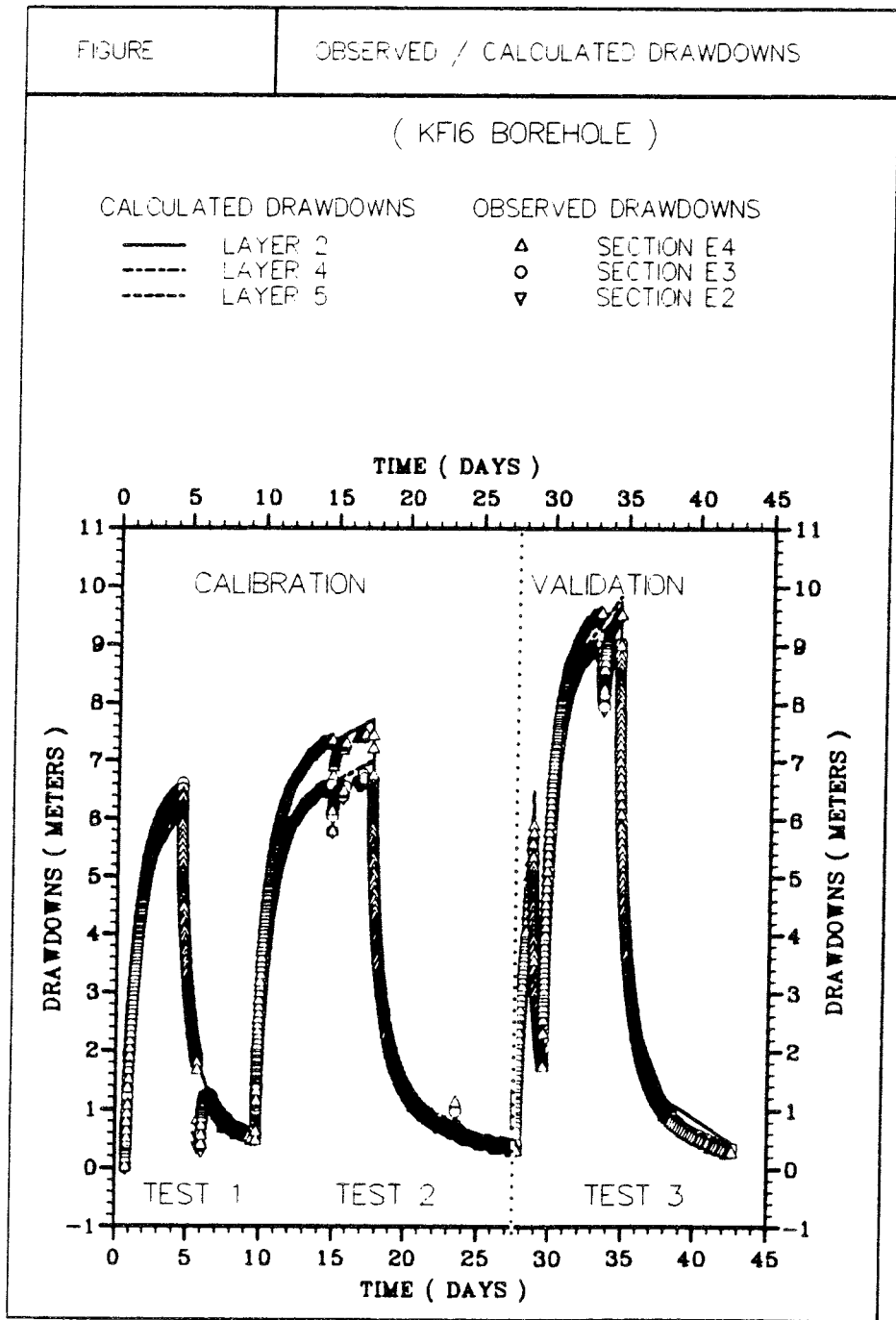


Figure 3-28. Comparison between measured and calculated drawdown in sections E2, E3 and E4 in borehole KFI06.

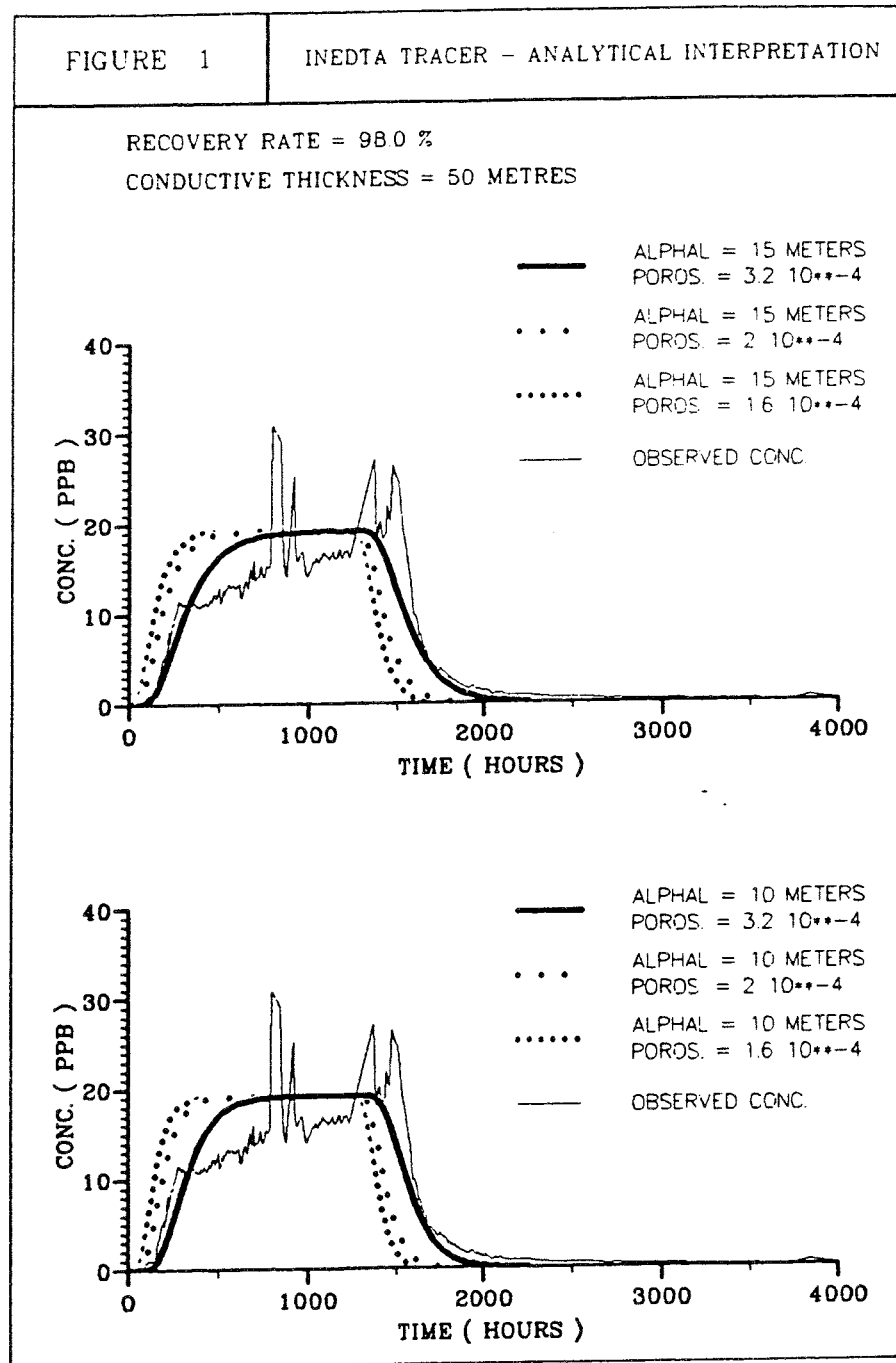


Figure 3-29. Analytical interpretation of tracer breakthrough in the upper test section (U) during the converging tracer test. Comparison between simulated results and field data.



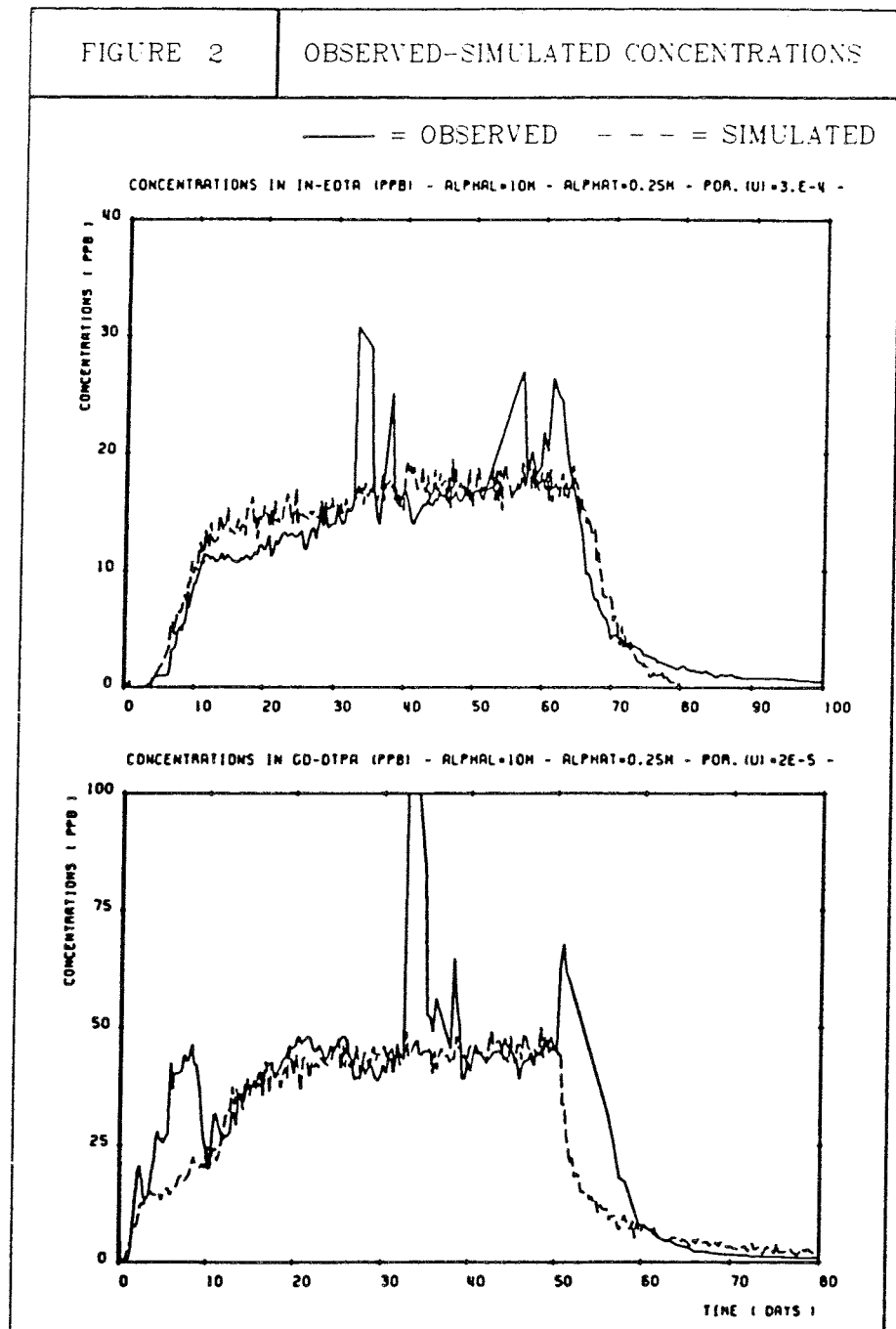


Figure 3-30. Numerical simulation of the converging tracer test. Comparison between measured (—) and simulated (---) concentrations for two of the four tracers injected in the upper section;

a) INEDTA:BF101(U), b) GDDTPA:KFI11(U)

## 3.9 UPV/ENRESA ANALYSIS

### 3.9.1 Modelling Objectives

An assumption of multiGaussianity inherently leads to a low degree of continuity in extreme values. If the parameter of interest is hydraulic conductivity and the processes studied are groundwater flow and mass transport, the absence of continuous paths of extreme values of hydraulic conductivity will have a retarding effect on the calculated travel times. In performance assessment studies addressing radionuclide release from a deep geological repository, underestimation in travel times may lead to decision making based on non-conservative results. This fact, and the fact that the multi-Gaussian model in most cases is selected simply because the supporting data are univariate Gaussian has formed the rationale for the study in which the impact of low continuity of extreme values on travel times is demonstrated by applying two stochastic models, one multiGaussian and one non-multi-Gaussian (the latter displaying high connectivity in extreme values) to a site similar to Finnsjön /Gómez-Hernández & Wen, 1993/.

It is shown that for a given univariate Gaussian histogram for  $Y = \log_{10} K$  and a covariance  $C_Y(h)$ , the latter which can be expressed as an integral of all possible indicator cross-covariances  $C_I(h; y, y')$ , there exist an infinity of combinations of indicator covariances that may yield a given  $Y$ -covariance, of which one set of combinations corresponds to a multiGaussian model ( $y$  and  $y'$  are arbitrary threshold values and  $h$  is the separation distance). Thus there exist other possible models which can reproduce the  $Y$ -covariance. The alternative model used in this study allows significant correlation ranges for indicator covariance corresponding to extreme values. This property is not possible to obtain for a multiGaussian model which renders independence between two indicators  $I(x; y)$  and  $I(x+h; y)$  as the threshold value  $y$  becomes extreme.

### 3.9.2 Modelling Approach

The area modelled with the two models is a vertical section through the Finnsjön site which features Zone 1, Zone 2 and the rock mass, c.f. Figure 3-31. The domain is 1000x1000m discretized into 50x50 cells of size 20x20m. The fracture zones are treated deterministically with constant hydraulic conductivities of  $10^{-4.5}$  and  $10^{-5.5}$  m/s, respectively. The boundary conditions imposed on the model will force groundwater to discharge at the outcrop of fracture zone 1. The hydraulic conductivity of the rock mass is modelled as a random function. The two models applied are univariate Gaussian with a mean  $\log_{10} K = Y$  equal to  $-8.0$  ( $\log_{10}$  m/s) and a variance equal to  $1$  ( $\log_{10}$  m/s)<sup>2</sup> and the same anisotropic covariance  $C_Y(h)$ . However the two models differ in their indicator covariances which have been defined for 9 thresholds (the nine deciles). Figure 3-32 shows the respective indicator correlograms (covariance normalized with respect to the indicator variance) for three thresholds. Worth pointing out is the high horizontal continu-

ity in the indicator variable for the last (90%) decile of the non-multi-Gaussian model which cannot be reproduced by a multiGaussian model.

Stochastic travel time analysis for particles released from an idealized repository, c.f. Figure 3-31, to the surface via fracture zone 1 was performed. Using the two models 200 unconditional realizations of  $Y$  were generated. Subsequently the two fracture zones were superimposed with constant geometry and material properties. Sequential simulation /Journel, 1989/ was used to generate realizations of rock mass conductivity. In the case of the multiGaussian model, GCOSIM3D /Gómez-Hernández, 1991/ was used and in the case of the non-multiGaussian model, ISIM3D /Gómez-Hernández & Srivastava, 1990/ was used. Two typical realizations based on the two models are shown in Figure 3-33. Subsequently groundwater flow and advective transport were simulated in the 200 realizations of each set, producing in each case 200 breakthrough curves of particle arrival at the outcrop of fracture zone 1 following (continuous) release of particles from a conceived repository area below Zone 2.

### 3.9.3 **Results**

The calculated breakthrough curves were used to construct bivariate cumulative probability distribution functions for arrival time and mass concentration, which enable assessment of the uncertainty in these two parameters, c.f. Figure 3-34. The results, for a given probability, show that the non-multi-Gaussian model gives higher concentrations in shorter time than that of the multiGaussian model. This implies that if a site is considered safe on the basis of uncertainty analysis using a multiGaussian model it may be labelled unsafe if the analysis is carried out using a non-multiGaussian model with high continuity of extreme high values.

### 3.9.4 **Conclusions**

In stochastic continuum modelling of flow and solute transport, the multi-Gaussian model is often chosen on the sole basis of the parsimony principle as the simplest model that can be described by a mean and a covariance.

An alternative, non-multiGaussian, model is presented. This model, with the same Gaussian histogram and covariance as the multiGaussian model shows a high continuity in extreme values. This fact renders the non-multiGaussian model to exhibit faster radionuclide transport than the multiGaussian model which cannot impose such a high continuity in the high values. The results show that probabilities of exceedence for small concentrations at given times is significantly higher for the non-multiGaussian model than for the multi-Gaussian model. Thus, the multiGaussian model is not a conservative model for nuclear waste disposal safety assessment.

Before selecting a multiGaussian model it is important to check not only that the data are univariate Gaussian, but also whether they are bivariate Gaus-

sian. A possible test is to calculate the indicator covariances for the actual data and compare them with the theoretical ones. If the test shows that the data are not bivariate Gaussian, alternative models must be used, such as the proposed indicator-based model. If the test turns out inconclusive, alternative models should at least be used as a complement to the multiGaussian model. The selection of the multiGaussian model should at any rate not be solely made on the basis of the parsimony principle.

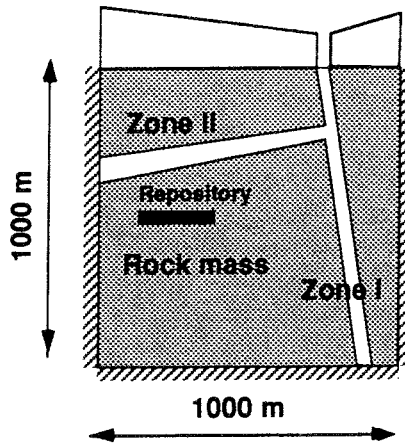


Figure 3-31. Geometry of flow model. Prescribed head boundary conditions used on the surface (vertical section).

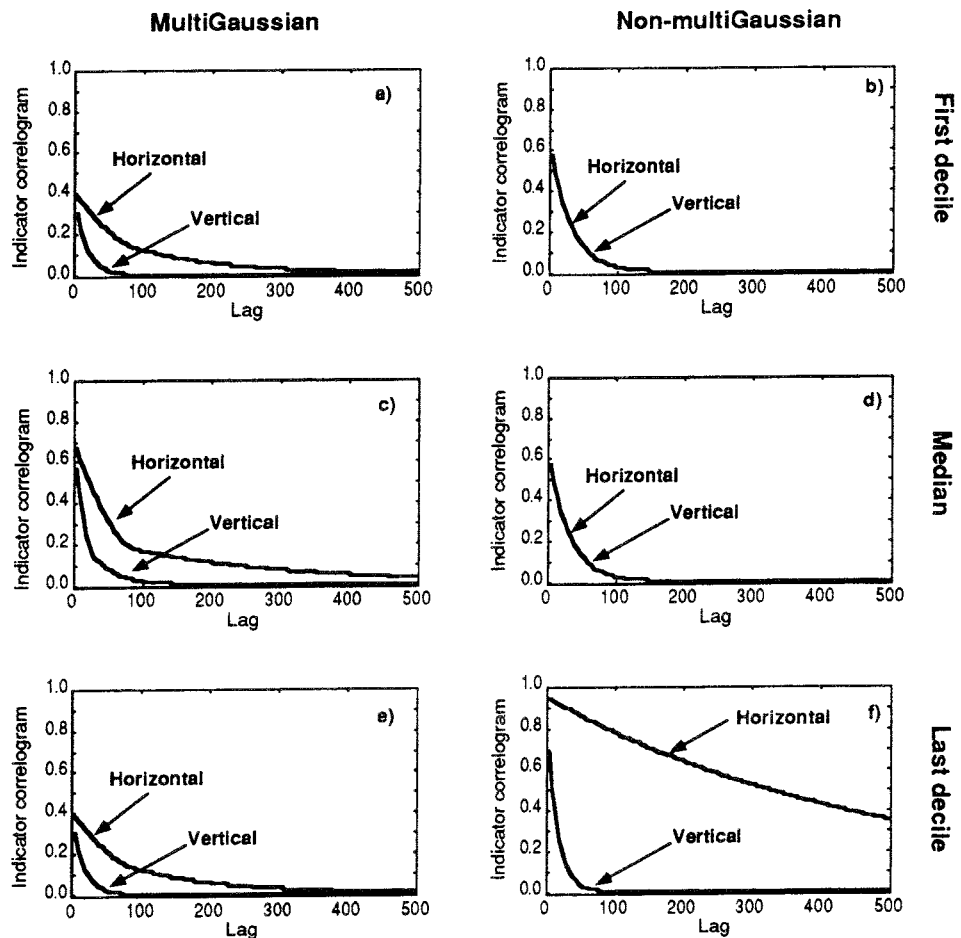


Figure 3-32. Indicator covariances for three selected thresholds for both the multiGaussian and the non-multiGaussian model.

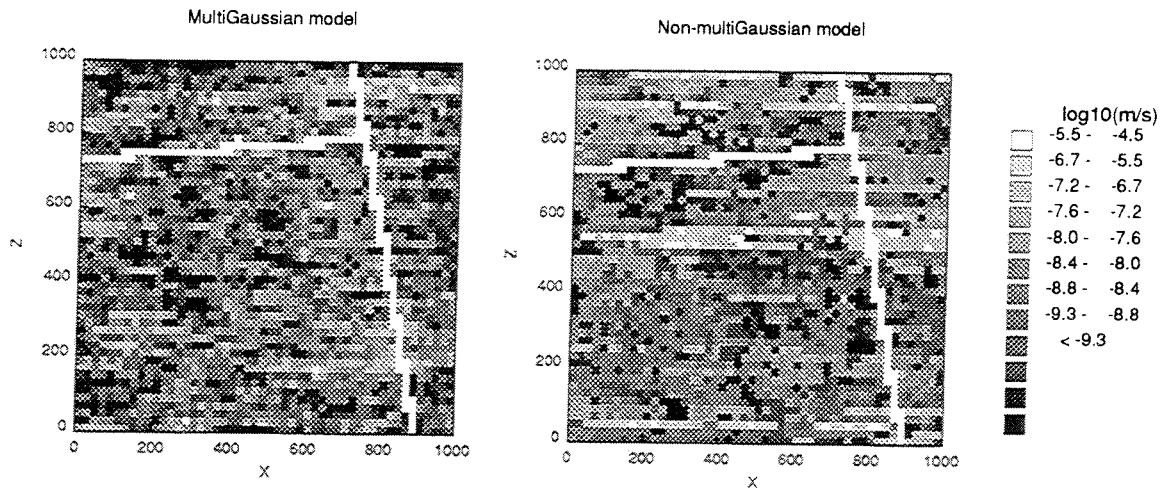


Figure 3-33. Typical realizations of hydraulic conductivity from the multiGaussian and non-multiGaussian model.

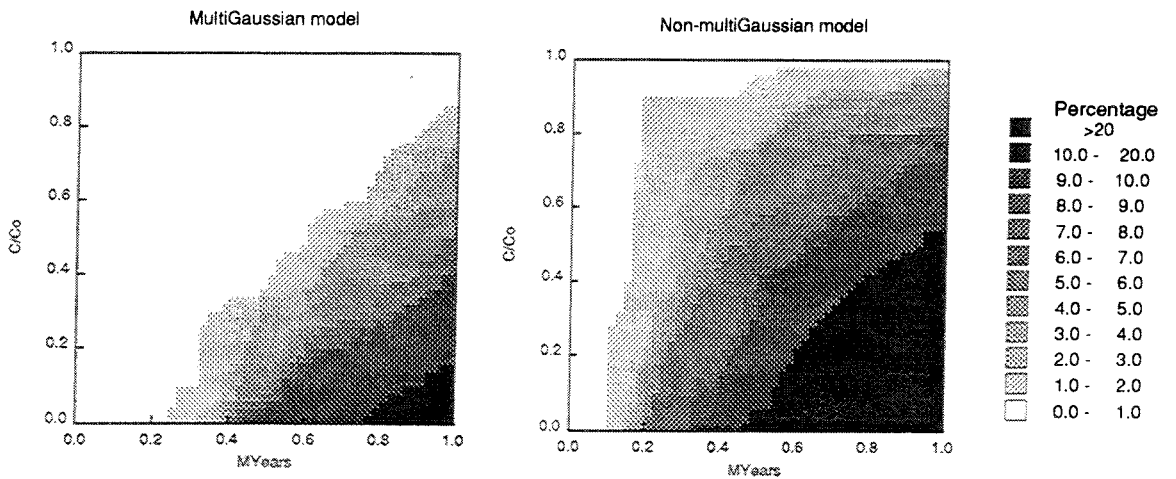


Figure 3-34. Bivariate cumulative probability distribution functions for mass concentration and arrival time (probability of concentration higher than a given value arriving at the surface before a given time).

## 4 COMPARATIVE DISCUSSION

### 4.1 **GENERAL**

The INTRAVAL Phase 2 analysis of the Finnsjön tracer experiments features results from nine different modelling teams using a variety of different approaches. Phase 1 constituted a first contact for the participating teams with the Finnsjön test data and some of these teams have continued their analysis during Phase 2. The Phase 2 results offer explicit attempts to validation of the set up models. A general observation is also that the dimensionality of some of the applications is three-dimensional and in addition stochastic approaches are employed, all of which are new ingredients compared to Phase 1.

Below some aspects of the approaches employed during the Phase 2 analysis of the Finnsjön tracer experiments are discussed and compared in more detail. These are; a) conceptual approaches employed, b) processes studied, c) scale of application, and d) the validation aspects of the studied problem.

### 4.2 **CONCEPTUAL APPROACHES**

The conceptual models applied by the modelling teams are also in Phase 2 of INTRAVAL focused on porous media approaches, c.f. Table 1-2. In Phase 1, five of the seven teams used porous media approaches while in Phase 2 seven of the nine teams used this concept. The two exceptions, in the latter case, are the VTT team, which uses a network of channels where transport is assumed to take place in a few non-interacting channels, and the Hazama team which uses a concept based on a representative elementary volume (REV) obtained through the Crack Tensor Theory.

Some of the teams have also compared different conceptual approaches. The PNC team uses two different ways to determine the hydraulic conductivity distribution and uses both one-dimensional stream tube and two-dimensional finite difference methods to analyze transport. The UPV team compares two stochastic models, Gaussian/non-Gaussian, and the PSI team applies both fracture and vein flow models. The U. of New Mexico team compares single- versus double porosity models. Some of the teams use the comparison to conclude which conceptual approach that gives the best correspondence to the experimental data and which of the models to be, at least partly, rejected.

The models used are mainly two-dimensional which is an obvious assumption given the two-dimensional character of flow in Zone 2. Some teams use one-dimensional transport concepts and two teams use three-dimensional

approaches. If all tracer tests are to be considered, a three-dimensional model may be needed, especially if the large scale head responses are to be incorporated. Experimental evidence of vertical interconnections between different subzones and leakage from the bedrock below the zone also speaks in favor of a three-dimensional approach. However, the relatively simple one-dimensional approaches may also be useful in some cases, like the radially converging test, where variations in source terms and effects of multiple flow paths and matrix diffusion are easily addressed. The dimensionality of the model does not seem to be decisive for the ability to reproduce the field responses at Finnsjön.

A major difference compared to Phase 1 is that geostatistical approaches have been introduced. In Phase 2 three modelling teams, Conterra/KTH-WRE, UPV, and Hazama, have used geostatistical methods to obtain transmissivity or aperture distributions for stochastic travel time analysis. Also the PNC team has initiated a geostatistical analysis of the Finnsjön data. These teams have demonstrated that stochastic approaches may be used within the context of a validation process, although the question remains how to formally validate a stochastic continuum model.

#### 4.3 PROCESSES STUDIED

In Phase 1 many of the teams studied several processes, trying to separate between them. However, one of the conclusions from Phase 1 was that the tracer experiments at Finnsjön may not be designed to discriminate between processes /Tsang & Neuman (editors), 1992/. The results were also somewhat ambiguous where e.g. matrix diffusion was considered to be important by one team while other teams considered it to have none or negligible effect.

In Phase 2, only four of the nine teams include more than one process, c.f. Table 1-2. The GEOSIGMA and PSI teams are the only teams which consider sorption. The reason for this is probably that there are no independent laboratory or field data for the weakly sorbing tracers used in the dipole test. It should also be noted that the PSI team uses a different data set from Finnsjön, previously used in INTRACOIN /SKI, 1986/, specially addressing sorption processes. The PSI team conclude that sorption parameters determined from these tests agree well with literature data.

The PSI team also made an analysis of the effect of matrix diffusion and came to the conclusion that matrix diffusion has a small but not negligible effect. The U. of New Mexico team also compares a single and a double porosity model and finds that very similar results are obtained and that no definite conclusion regarding matrix diffusion can be drawn although they claim that matrix diffusion is an important process at Finnsjön based on the ratio of fracture to matrix porosity. The GEOSIGMA team draw the opposite conclusion based on the same ratio and therefore they did not consider matrix diffusion at all in their analysis.

In the stochastic continuum approaches, transport is treated as purely ad-

vective and these models were designed for other purposes than process discrimination.

The general conclusion drawn by all teams is that flow and transport in Zone 2 is governed by advection and that hydrodynamic dispersion also is needed to explain the breakthrough curves. The question whether matrix diffusion is important in these experiments or not, still remains open, although most teams agree that matrix diffusion has no, or very small, effect given the high induced velocities and low ratio of fracture to matrix porosity.

#### 4.4 SCALE OF APPLICATION

The tracer tests performed at Finnsjön have been conducted in a well-defined borehole array. Thus the experiment scale is also well defined, being on the order of 200x200 m. During Phase 1 mostly analytical tools were employed thus focusing in specifically on the experimental scale. During Phase 2, however, numerical applications dominate and the scale considered is in some instances on the order of 1000x1000m, c.f. Table 4-1. This is particularly true for the two stochastic continuum applications which both address transport phenomena on scales larger than the actual experiment scale. Taking scale alone into consideration, the results of most modelling teams can be directly compared.

#### 4.5 VALIDATION ASPECTS

The classical approach to model validation in hydrogeology is calibration of a set of model parameters against a given experiment geometry in a given geological domain for a specific stress of the system. The validation constitutes prediction of model behavior for another experiment condition (altered stress and/or geometry) in the same geological domain and comparison with field data.

During Phase 1, only three out of seven modelling teams (EdM, GEOSIGMA (formerly SGAB) and JAERI) formally addressed this classical type of validation by first calibrating their model with the radially converging test and subsequently predicting the dipole test /Tsang & Neuman (editors), 1992/. The EdM team used a multiple channel model and explicitly addressed validation and claimed proper process and parameter identification but acknowledged poor representation of horizontal heterogeneity. The JAERI team did not explicitly address validation but utilized the parameter set obtained from the calibration of the radially converging test to predict the dipole test. GEOSIGMA was the responsible field organization which conducted and interpreted the field tests conducted at Finnsjön. The GEOSIGMA team in succession used the collected field data to enhance their descriptive models, used that information to predict the subsequent tracer test, and finally attempted and succeeded well to predict the dipole test response.



During Phase 2, various validation aspects have been considered, c.f. Table 4-1. Five groups address the classical approach to validation, whereas two groups utilizing the stochastic continuum approach address other validation aspects.

The modelling teams from GEOSIGMA and VTT address parameter consistency between all three tracer tests performed at Finnsjön (including the preliminary tracer test during interference testing). The results show that the average transport behavior can be acceptably described with one single set of transport parameters. However, for a detailed understanding of individual transport routes, transport parameters need to be adjusted for different flow geometries. The PNC team utilizes a porous medium, double porosity model to calibrate the transport parameters to the dipole tracer test. The validity of the model was subsequently checked by simulating the radially converging test. The results showed good predictive capability for early times whereas tails in the breakthrough curves are poorly represented. The alternate sequence used by the PNC team, in that they start out with the dipole test in their analysis, may have helped to get a better understanding of the heterogeneity between BFI01 and BFI02. The BRGM team uses the classical approach and succeeds in predicting later interference test results based on calibrations of early interference tests. The U. of New Mexico team uses a single/double porosity 2D model (in vertical sections) to predict the converging test and checks the validity of their model/s by simulating the dipole test. They conclude that a reasonable agreement between measured and simulated breakthrough is obtained.

The Conterra/KTH-WRE team addresses a performance assessment issue, that of extrapolation of transport models calibrated on a small scale to larger transport scales. Using an exhaustive reference transmissivity field and the stochastic continuum approach they show that a model calibrated on an experimental scale is not validated on a far-field scale when being subjected to extrapolation and simulation of a far-field natural gradient test. The reason being that the local scale conditioning data do not suffice also to describe far-field scale heterogeneity.

With the more and more frequent use of stochastic continuum models the UPV team raises an important issue relating to the inherent choice of statistical model when generating hydraulic conductivity/transmissivity fields. The bottom line of the UPV work is that when and if the multiGaussian model is used this should be preceded by a check whether the data also are bivariate Gaussian and with the understanding that the multiGaussian approach intrinsically suppresses connectivity of extreme values. The latter is of paramount interest from a performance assessment perspective since an unwarranted use of the multiGaussian model may transform an "unsafe" site to a "safe" one.

In summary the approaches on model validation are versatile and focus in on other issues than the classical validation issue, which may be equally important in improving our predictive capability of solute transport phenomena in crystalline rock.

Table 4-1. Phase 2 analysis of tracer tests at Finnsjön. Scale of problem and validation aspect of problem studied.

Modelling team	Scale of problem	Validation aspects of problem
Hazama Corp., Japan	1000x1000x100m (far-field) 300x300x100m (local scale) 20x20x20m discr.	
Conterra/KTH-WRE (SKB), Sweden	1200x1200m (far-field) 200x200m (local scale) 20x20m discr.	Extrapolation of a model, calibrated on a local scale to the far-field scale.
BRGM/ANDRA, France	2500x1200x100m	Flow parameters ( $K$ and $S_s$ ), transport parameters ( $n$ , $\alpha_L$ , $\alpha_T$ ) (not completed).
GEOSIGMA, Sweden	2500x1500m (far-field) 500x500m (local scale) 10x10m discr.	Same conceptual model used for all analyzed tracer tests. Check whether it is possible to recreate tracer tests results in various geometries with the same transport parameters.
VTT (TVO), Finland	< 200m	Same conceptual model possible to explain all tracer test results.
PNC, Japan	< 200m	Calibrated dipole model tested by simulating the radially converging tracer test.
UPV (ENRESA), Spain	1000x1000m 20x20m discr.	Use of Gaussian model based on parsimony. Conservative choice!?
PSI (NAGRA), Switzerland	~ 30m	Consistency in evaluated transport parameters. Comparison between laboratory test results with field test results in granitic rocks performed at different sites and in various geometries.
U. of New Mexico, U.S.A.	~ 200x200m	Model(-s) calibrated using the radially converging tracer test are tested by simulating the dipole tracer test.

**REFERENCES**

- Ababou, R., Sagar, B., and Wittmeyer, G. 1992 : Testing procedure for Spatially Distributed Flow Models. *Adv. Water Res.*, vol. 2 of special issue on model validation, 1992.
- Ahlbom, K., Andersson, P., Ekman, L., Gustafsson, E., Smellie, J., and Tullborg, E-L. 1986 : Preliminary investigations of fracture zones in the Brändan area, Finnsjön study site. SKB Technical Report TR 86-05.
- Ahlbom, K., Andersson, P., Ekman, L., and Tirén, S. 1988 : Characterization of fracture zones in the Brändan area, Finnsjön study site. SKB Progress Report AR 88-09.
- Ahlbom, K., and Smellie, J.A.T. (editors) 1989 : Characterization of fracture zone 2, Finnsjön study site, Part 1-6. SKB Technical Report TR 89-19.
- Andersson, J-E., Ekman, L., Gustafsson, E., Nordqvist, R. and Tirén, S. 1989 : Hydraulic Interference Tests and Tracer Tests within the Brändan Area, Finnsjön Study Site - The Fracture Zone Project Phase 3. SKB Technical Report TR 89-12.
- Andersson, P., Eriksson, C-O., Gustafsson, E., and Ittner, T. 1990 : Dipole Tracer Experiment in a Low-Angle Fracture Zone at the Finnsjön Site, Central Sweden- Experimental Design and Preliminary Results. SKB Progress Report AR 90-24.
- Andersson, P., Nordqvist, R., Persson, T., Eriksson, C-O., Gustafsson, E., and Ittner, T. 1993 : Dipole Tracer Experiment in a Low-Angle Fracture Zone at Finnsjön - Results and interpretation. The Fracture Zone Project - Phase 3. SKB Technical Report 93-26.
- Andersson, P. (ed.) 1993 : The Fracture Zone Project - Final Report. SKB Technical Report TR 93-20.
- Gidlund, J., Moreno, M., and Neretnieks, I. 1990 : Porosity and diffusivity measurements of samples from Finnsjön. SKB Progress Report AR 90-34.
- Gómez-Hernández, J.J., and Srivastava, R.M. 1990 : ISIM3D: an ANSI-C Three-dimensional Multiple Indicator Conditional Simulation Program. *Computers and Geosciences*, vol. 16, no. 4, pp. 395-440.

- Gómez-Hernández, J.J. 1991 : A Stochastic Approach to the Simulation of Block Conductivity Values Conditioned upon Data Measured at a Smaller Scale. PhD Thesis, Stanford University, U.S.A.
- Gómez-Hernández, J.J. and Wen, X-H. 1993 : MultiGaussian Models – The Danger of Parsimony, In Proc. of Int. Workshop on Statistics of Spatial Processes: Theory and Applications, Bari, Italy, 27–30 Sept 1993.
- Gustafsson, E., and Klockars, C-E. 1981 : Studies on groundwater transport in fractured crystalline rock under controlled conditions using non-radioactive tracers. SKBF/KBS Technical Report TR 81-07.
- Gustafsson, E., and Klockars, C-E. 1984 : Study of strontium and cesium migration in fractured crystalline rock. SKBF/KBS Technical Report TR 84-07.
- Gustafsson, E., Andersson, P., Eriksson, C-O., and Nordqvist, R. 1990 : Radially Converging Tracer Experiment in a Low Angle Fracture Zone at the Finnsjön Site, Central Sweden. The Fracture Zone Project Phase 3. SKB Progress Report AR 90-27.
- Gustafsson, E., and Andersson, P. 1991 : Groundwater flow conditions in a low-angle fracture zone at Finnsjön, Sweden. Journal of hydrology, Vol 126, pp 79-111.
- Gustafsson, E., and Nordqvist, R. 1993 : Radially Converging Tracer Experiment in a Low Angle Fracture Zone at the Finnsjön Site, Central Sweden. The Fracture Zone Project Phase 3. SKB Technical Report 93-25.
- Hatanaka, K., and Mukai, S. 1993a : Preliminary Modelling of the Effect of Heterogeneity on Tracer Transport at Finnsjön Site. Presentation at the third INTRAVAL Phase 2 Workshop, San Antonio, Texas, November 9-13, 1992.
- Hatanaka, K., and Mukai, S. 1993b : Study on Estimation of Hydraulic Conductivity and Tracer Transport at Finnsjön Site. Presentation at the Fourth INTRAVAL Phase 2 Workshop, Stockholm, Sweden, August 30-September 3, 1993.
- Hautojärvi, A., and Taivassalo, V. 1988 : INTRAVAL PROJECT. Test case 5: Tracer tests at Finnsjön. Predictive modelling of the radially converging experiment. Report YJT-88-13.
- Hautojärvi, A., and Coworkers. 1992 : VTT Analysis of Tracer Data. In Tsang and Neuman (editors). The International INTRAVAL Project. NEA/SKI 1992.

- Hautojärvi, A. 1993 : Summary of VTT analysis of Finnsjön. Presentation at the INTRAVAL Phase II Working Group 2 meeting, Berkeley, California, 15–16/3, 1993.
- Jakob, A., and Hadermann, J. 1993 : INTRAVAL Finnsjön Test – modeling results for some tracer experiments. PSI-Bericht in prep.
- Journel, A.G. 1989 : Fundamentals of Geostatistics in Five Lessons, volume 8 of Short Courses in Geology. AGU, Washington D.C.
- Kobayashi, A., and Yamashita, R. 1993 : Heterogeneous Anisotropic Model of Finnsjön Test Case and Seepage and Transport Analyses for Radial Converging Test. Presentation at the Fourth INTRAVAL Phase 2 Workshop, Stockholm, Sweden, August 30–September 3, 1993.
- Kung, C-S., Cvetkovic, V., and Winberg, A. 1992b : Calibration and Validation of a Stochastic Continuum Model using the Finnsjön Dipole Tracer Test. A Contribution to INTRAVAL Phase 2. SKB Technical Report TR 92–35.
- Luis, S. and McLaughlin, D. 1992 : A Stochastic Approach to Model Validation. Adv. Water Res., vol. 1 of special issue on model validation, 1992.
- Ng, T-T., and Kota, S. 1993 : Interpretation of the Radially Converging Tracer Tests at the Finnsjön Research Site, Sweden. U. of New Mexico Report in prep.
- Schwartz, J., Fillon, E., Sauty, J.P., and Dewiere, L. 1993 : FINNSJÖN SITE (SWEDEN) – Interpretation of Interference Tests. In : Proceedings International High Level Radioactive Waste Management Conference, Las Vegas, April 26–30, 1993.
- Schwartz, J. 1993 : Participation au test INTRAVAL – Finnsjön – Interprétation des tests de traçage en milieu granitique – Modélisation du test de traçage en radial convergent – Rapport de synthèse. ANDRA report 663 RP BRG 93–014.
- SKI 1986 : INTRACOIN Final Report Levels 2 and 3. SKI Report 86:2.
- SKI/NEA 1990 : The International INTRAVAL Project. Background and Results. OECD Paris 1990.
- Thiery, D. 1990 : Logiciel MARTHE – Modélisation d'Aquifères par Maillage Rectangulaire en Régime Transitoire pour le calcul Hydrodynamique des Ecoulements – Release 4.3. BRGM Report no. 32210.
- Travis, B.J., and Birdsell K.H. 1991 : TRACR3D: A model of flow and transport in Porous media. Model description and user's manual. LA-11798-M, Los Alamos.

- Tsang, C-F, and Neuman, S. (editors) 1992 : The International Intraval Project. Phase 1, Test Case 5. Studies of Tracer Experiments in a Fracture Zone at the Finnsjön Research area. NEA/SKI, OECD Paris 1992.
- Van Genuchten, M.Th., and Alves, W.J. 1982 : Analytical solutions of the one-dimensional convective-dispersive solute transport equation, U. S. Dep. Agric. Tech. Bull., 1661.
- Voss, C.I. 1990 : SUTRA - A finite-element simulation model for saturated-unsaturated, fluid-density-dependent groundwater flow with energy transport or chemically-reactive single-species solute transport. Version V06902D. U.S. Geological Survey Water-Resources Investigations Report 84-4369.

# List of SKB reports

## Annual Reports

1977-78

TR 121

### **KBS Technical Reports 1 – 120**

Summaries

Stockholm, May 1979

1979

TR 79-28

### **The KBS Annual Report 1979**

KBS Technical Reports 79-01 – 79-27

Summaries

Stockholm, March 1980

1980

TR 80-26

### **The KBS Annual Report 1980**

KBS Technical Reports 80-01 – 80-25

Summaries

Stockholm, March 1981

1981

TR 81-17

### **The KBS Annual Report 1981**

KBS Technical Reports 81-01 – 81-16

Summaries

Stockholm, April 1982

1982

TR 82-28

### **The KBS Annual Report 1982**

KBS Technical Reports 82-01 – 82-27

Summaries

Stockholm, July 1983

1983

TR 83-77

### **The KBS Annual Report 1983**

KBS Technical Reports 83-01 – 83-76

Summaries

Stockholm, June 1984

1984

TR 85-01

### **Annual Research and Development Report 1984**

Including Summaries of Technical Reports Issued during 1984. (Technical Reports 84-01 – 84-19)

Stockholm, June 1985

1985

TR 85-20

### **Annual Research and Development Report 1985**

Including Summaries of Technical Reports Issued during 1985. (Technical Reports 85-01 – 85-19)

Stockholm, May 1986

1986

TR 86-31

### **SKB Annual Report 1986**

Including Summaries of Technical Reports Issued during 1986

Stockholm, May 1987

1987

TR 87-33

### **SKB Annual Report 1987**

Including Summaries of Technical Reports Issued during 1987

Stockholm, May 1988

1988

TR 88-32

### **SKB Annual Report 1988**

Including Summaries of Technical Reports Issued during 1988

Stockholm, May 1989

1989

TR 89-40

### **SKB Annual Report 1989**

Including Summaries of Technical Reports Issued during 1989

Stockholm, May 1990

1990

TR 90-46

### **SKB Annual Report 1990**

Including Summaries of Technical Reports Issued during 1990

Stockholm, May 1991

1991

TR 91-64

### **SKB Annual Report 1991**

Including Summaries of Technical Reports Issued during 1991

Stockholm, April 1992

1992

TR 92-46

### **SKB Annual Report 1992**

Including Summaries of Technical Reports Issued during 1992

Stockholm, May 1993

## Technical Reports

### List of SKB Technical Reports 1994

TR 94-01

#### **Anaerobic oxidation of carbon steel in granitic groundwaters: A review of the relevant literature**

N Platts, D J Blackwood, C C Naish  
AEA Technology, UK  
February 1994

TR 94-02

#### **Time evolution of dissolved oxygen and redox conditions in a HLW repository**

Paul Wersin, Kastriot Spahiu, Jordi Bruno  
MBT Tecnología Ambiental, Cerdanyola, Spain  
February 1994

TR 94-03

#### **Reassessment of seismic reflection data from the Finnsjön study site and prospectives for future surveys**

Calin Cosma<sup>1</sup>, Christopher Juhlin<sup>2</sup>, Olle Olsson<sup>3</sup>  
<sup>1</sup> Vibrometric Oy, Helsinki, Finland  
<sup>2</sup> Section for Solid Earth Physics, Department of Geophysics, Uppsala University, Sweden  
<sup>3</sup> Conterra AB, Uppsala, Sweden  
February 1994

TR 94-04

#### **Final report of the AECL/SKB Cigar Lake Analog Study**

Jan Cramer<sup>1</sup>, John Smellie<sup>2</sup>  
<sup>1</sup> AECL, Canada  
<sup>2</sup> SKB, Sweden  
May 1994

TR 94-05

#### **Tectonic regimes in the Baltic Shield during the last 1200 Ma - A review**

Sven Åke Larsson<sup>1,2</sup>, Eva-Lena Tullborg<sup>2</sup>  
<sup>1</sup> Department of Geology, Chalmers University of Technology/Göteborg University  
<sup>2</sup> Terralogica AB  
November 1993

TR 94-06

#### **First workshop on design and construction of deep repositories - Theme: Excavation through waterconducting major fracture zones Såstaholm Sweden, March 30-31 1993**

Göran Bäckblom (ed.),  
Christer Svemar (ed.)  
Swedish Nuclear Fuel & Waste Management Co,  
SKB  
January 1994